ADDIS ABABA UNIVERSITY

ADDIS ABABA INSTITUTE OF TECHNOLOGY

SCHOOL OF CIVIL AND ENVIRONMENTAL ENGINEERING

EVALUATION OF REINFORCEMENT DETAILING IN CORNER BEAM-COLUMN JOINTS

A Thesis in structural Engineering

By Linda Getachew

November, 2018

Addis Ababa

A Thesis

Submitted in Partial Fulfillment of the Requirements for the Degree of Master of Science

The undersigned have examined the thesis entitled '**Evaluation of Reinforcement Detailing in Corner Beam-Column Joints**' presented by **Linda Getachew**, a candidate for the degree of **Master of Science** and hereby certify that it is worthy of acceptance.

Dr. Ing. Girma Zerayohannes		
Advisor	Signature	Date
Dr. Ing. Adil Zekaria		
Internal Examiner	Signature	Date
Dr. Abrham Gebre		
External Examiner	Signature	Date
Dr. Agizew Nigussie		
Dean, SCEE	Signature	Date

ACKNOWLEDGMENT

First and foremost, I would like to thank God for giving me the strength to carry out this thesis. This study was conducted under the supervision of Dr. Ing. Girma Zerayohannes. I would like to express my deepest gratitude for the support and guidance that he has provided me throughout the study. Finally, I would like to thank my family and friends for always supporting me.

Table of Contents

ACKNOWLEDGMENT i
LIST OF FIGURES iv
LIST OF TABLES vi
ABSTRACT ix
1. Introduction 1
1.1 Background 1
1.2 Statement of the problem 2
1.3. Objective of the study 3
1.3.1 General objective 3
1.3.2 Specific objectives 3
1.4. Scope of the study 3
1.5. Outline of the Study 3
2. Literature review 5
2.1 Strut and Tie Model 5
2.1.1 Background on strut and tie modelling 5
2.1.2 Design steps of disturbed regions by strut and tie model (STM) 7
2.1.3 Components of strut and tie model 7
2.1.3.1 Struts 8
2.1.3.2 Ties 10
2.1.3.3 Nodes 11
2.1.3.4 Dimensioning strut and tie components 12
2.2. Reinforcement detailing in frame corners 13
2.2.1 Introduction 13
2.2.2 Failure modes of concrete joints 14
2.2.3 Definition of corner efficiency 15
2.2.4 Requirements in Eurocode 2 16
2.2.5 Behavior of different corner joint details 17
2.2.5.1. Impact of reinforcement ratio on corner joint efficiency 22
3. Analytical Design using strut-and-tie model 24
3.1 Input data for frame corners 24
3.2 Strut and tie scheme 24
3.2.1 Strut and tie analysis of the joint, scheme-1 25
3.2.2 Strut and tie analysis of the joint, scheme -2 34

3.3 Moment capacity of the member 38
4. Nonlinear Finite Element Analysis of a Corner Joint 40
4.1 VecTor2 Analytical Procedure 40
4.1.1 Concrete 41
4.1.2 Steel Rebar 41
4.1.3 Geometry and Meshing 42
4.2 verification 43
4. 3 Finite Element Analysis of the corner joint 47
4.3.1 Preliminary study 49
4.3.2 Focus on thesis variants 51
4.3.2.1 Reinforcement layout 1 (RL1) 52
4.3.2.2 Reinforcement layout 2 (RL2) 54
4.3.2.3 Reinforcement layout 3 (RL3) 55
4.3.2.4 Reinforcement layout 4 (RL4) 56
4.3.3 Corner Joints with Chamfer 57
4.3.4 Effect of reinforcement ratio 60
4.4 Discussions of results 63
5. Conclusion and recommendation 66
5.1 conclusion 66
5.2 Recommendation 66
References 67
Appendix 71
A. Effect of reinforcement ratio on corner efficiency 71

LIST OF FIGURES

Figure 2. 1 Examples of division of B and D regions in common structures (Tjhin and Kuchma, 2002). 5
Figure 2. 2 Illustration of St. Venant's principle (FHWA, 2006). 6
Figure 2. 3 Flowchart illustrating STM steps. (Brown et al. 2008) 7
Figure 2. 4 Strut and tie model (for illustration) 8
Figure 2. 5 Cracks in bottle-shaped strut from transverse tensile stress (Nilson, Darwin and Dolan, 2004) 8
Figure 2. 6 Partial discontinuity (a) and full discontinuity (b) regions arising from compression stress (Westberg, 2010) 9
Figure 2. 7 Design strength of concrete strut (no transverse tension), EC2 10
Figure 2. 8 Concrete strut with transverse tension 10
Figure 2. 9 Classification of nodes 11
Figure 2. 10 Hydrostatic and Non-Hydrostatic nodes 12
Figure 2. 11 structures subjected to opening and closing moments (Campana et al. 2013) 14
Figure 2. 12 Stresses σ_x and σ_y in a right-angled corner subjected to opening moment (Moretti, 2014) 14
Figure 2. 13 Diagonal tensile failure illustration (Hsu and Mo, 2010) 15
Figure 2. 14 Frame corner with moderate opening moment (Eurocode 2) 16
Figure 2. 15 Frame corner with large opening moment (Eurocode 2) 16
Figure 2. 16 Test Specimens of Nilsson (1973) 18
Figure 2. 17 Recommended detail by Nilsson (1973) 18
Figure 2. 18 Type 1 and Type 2 detailing tested by Johansson (2000) 20
Figure 2. 19 Detailing of Opening Corners Recommended by Bureau of Indian Standards (1999) 20
Figure 2. 20 Detailing of Wall Intersections and Corners Recommended by ACI 315-92. 21

Figure 3. 1 Sample D-region of a corner joint 24
Figure 3. 2 proposed strut and tie models 25
Figure 3. 3 Delineated D-region of a beam-column joint (scheme-1) 25
Figure 3. 4 Resultant forces acting on D-region (scheme-1) 26
Figure 3. 5 Proposed strut and tie model for scheme-1 26
Figure 3. 6 Internal forces in strut and tie model (scheme-1) 27
Figure 3. 7 Forces acting on Node B 28
Figure 3. 8 forces acting on Node F 30
Figure 3. 9 Dimensions of the bottle-shaped strut BC 32
Figure 3. 10 Reinforcing bars for RL1 Figure 3. 11 Reinforcing bars for RL2 33
Figure 3. 12 Delineated D-region of a beam-column joint (scheme-2) 34
Figure 3. 13 Resultant forces acting on D-region (scheme-2) 34
Figure 3. 14 Proposed strut and tie model for scheme-2 35
Figure 3. 15 Internal forces in strut and tie model (scheme-2) 35
Figure 3. 16 Reinforcing bars for RL3 38
Figure 3. 17 Reinforcing bars for RL4 38

Figure 4. 1 Element mesh and different material regions in VecTor2 42
Figure 4. 2 Loading arrangement of the test specimens by Roshan et al. (2015) 43
Figure 4. 3 Dimensions and method of loading of test model for Nabil et al. (2014) 43

Figure 4. 4 Loading arrangement of the Nilsson's (1973) test specimens 44
Figure 4. 5 Reinforcement details by Roshan et al. (2015) 44
Figure 4. 6 Reinforcement details by Nabil et al. (2014) 44
Figure 4. 7 Nilsson's (1973) reinforcement details 45
Figure 4. 8 Model for F1 45
Figure 4. 9 Model for F4 45
Figure 4. 10 Model for SP1 45
Figure 4. 11 Model for SP2 45
Figure 4. 12 comparison of results of FE and tests for F1 of Nabil et al. (2014) 46
Figure 4. 13 geometrical model used for FEM (dimensions are in mm) 48
Figure 4. 14 Reinforcement layout in earlier practice 49
Figure 4. 15 Load displacemet diagram for preliminary joint 50
Figure 4. 16 a) crack pattern for the preliminary model b) crack pattern for such reinforcement according to Nilsson (1973) 51
Figure 4. 17 Evaluated structural details for corner joints. 52
Figure 4. 18 Maximum principal strain, ε_1 53
Figure 4. 19 Crack pattern at Failure, RL1 53
Figure 4. 20 Crack pattern at Failure, RL2 54
Figure 4. 21 crack pattern at failure, RL3 56
Figure 4. 22 a) crack pattern by Johansson (2001) b) crack pattern of RL4 57
Figure 4. 23 comparison of load carrying capacity 57
Figure 4. 24 Corner joint with chamfer 58
Figure 4. 25: variation of σ_x along the diagonal for varying chamfer sizes 58
Figure 4. 26 Load displacement diagram of chamfered corners 59
Figure 4. 27 Crack location of chamfered corners 60
Figure 4. 28 Load Deflection relationship of RL1 with varying percentage of tensile reinforcement . 61
Figure 4. 29 Load Deflection relationship of RL2 with varying percentage of tensile reinforcement . 61
Figure 4. 30 Load Deflection relationship of RL2 with varying percentage of tensile reinforcement . 62
Figure 4. 31Load Deflection relationship of RL4 with varying percentage of tensile reinforcement .. 62
Figure 4. 32 Force-displacement diagram for RL1 and RL2 63
Figure 4. 33 Force-displacement diagram for RL3 and RL4 64

LIST OF TABLES

Table 2. 1 Dimensioning of struts for scheme-1 31
Table 2. 2 Dimensioning of nodes for scheme-1 31
Table 2. 3 Dimensioning of struts for scheme-2 35
Table 2. 4 Dimensioning of nodes for scheme-2 36

Table 4. 1: Material Behavior Models for Concrete 41
Table 4. 2 Material Behavior Models for Reinforcement 42
Table 4. 3 FEM results of reinforcement details by Roshan et al. (2015) 46
Table 4. 4 FEM results of reinforcement details by M. Nabil et al. (2014) 46
Table 4. 5 FEM results of reinforcement details by Nillson's (1973) 46
Table 4. 6 Models designation and their properties 47
Table 4. 7 Results of chamfered corners 59

NOTATIONS

Roman upper case letters

A_s	reinforcement area
C	compressive force
E	Young's modulus
E_c	Young's modulus of concrete
E_s	Young's modulus of reinforcement
F	load
F_c	compressive force
F_s	tensile force
F_R	resisting force
G_F	fracture energy
L	length
M_A	moment in section A
M_B	moment in section B
M_{UT}	test ultimate moment
M_{cal}	theoretical Ultimate Moment of Resistance of the Design Section.
M_{uv}	ultimate moment in VecTor2
P	load

Roman lower case letters

b	width
d	effective height
f_{ck}	compressive cylinder strength of concrete
$f_{c,cube}$	compressive cube strength of concrete
f_{yd}	yield strength of reinforcement
f_{ctd}	tensile strength of concrete
f_{yk}	characteristic yield strength of reinforcement
k	stiffness

Greek letters

ΔF	load increment
ε	Strain rate
ε_c	concrete strain
ε_s	reinforcement strain
ε_u	ultimate concrete strain in tension
θ	angle between cracks
ρ	reinforcement ratio,
σ	stress
σ_1, σ_2	principal stresses
σ_c	concrete stress
σ_s	reinforcement stress
σ_{sp}	tensile strength
σ_x	tensile stress in x-direction
σ_y	tensile stress in y-direction
τ	shear stress
ϕ	bar diameter
ν	poisson's ratio
ω_s	mechanical reinforcement ratio
γ_c	partial safety factor for concrete
γ_s	partial safety factor for steel

ABSTRACT

Structural joints in a rigid frame should be capable of sustaining forces higher than those of the connecting members. However, while beams and columns are designed and detailed with considerable care, the same cannot be said about the joints in RC rigid frames. The structural behavior will be different from that assumed in the analysis and design, if the joints are incapable of sustaining the forces and deformations induced due to the transfer of forces among the members meeting at the joint.

A key objective in structural design is to produce structures that have adequate capacity for the load they would be subjected to in their design life. So, how does the reinforcement detailing aid or prevent the achievement of this objective? In this thesis, a study is undertaken into the detailing aspects of reinforced concrete structures. This paper presents a critical review of recommendations regarding the detailing of corner joints subjected to opening moments as per Eurocode 2. The work includes the finite element analysis of four recommended detailing systems in the Eurocode namely, loop reinforcement, hairpin reinforcement with stirrups, hairpin reinforcement with stirrups and diagonal bars and loop reinforcement with diagonal bars. In addition, the effect of different sizes of chamfer at the reentrant corner and the effect of different percentage of tensile steel are studied.

The finite element analysis consisted of simulating portal type opening corners made of normal strength concrete under monotonically increasing static loads. Some aspects of the structural behavior studied include the stress and strain distribution in the concrete, cracking moment, crack pattern and corner efficiency. From the study, it was concluded that all except the detailing with hairpin reinforcement with stirrups and diagonal bars, were unable to reach full capacity. In addition, it is suggested that the reinforcement ratio limit set in the Eurocode 2 be revised.

This study is not enough to evaluate the detailing of corner joints subjected to opening moments. It is highly suggested that a laboratory investigation be conducted in order to accurately test the corner capacity as its accuracy betters software simulations.

1. Introduction

1.1 Background

Many reinforced concrete failures occur not because of any inadequacies in the analysis of the structure or in design of the members but because of inadequate attention to the detailing of reinforcement (Nilsson, 1973). The beams and columns in a framed structure are designed based on simple element theories as the design principles for these basic elements are well understood. The same theory is invariably extended to the design of joints connecting these basic elements. The beam face of a joint is designed as a beam and the column face of the joint is designed as a column. The assumption that the joint is rigid, is probably an over simplification and may have been made for the purpose of design convenience. In fact, the behavior of joints is quite complex and thus the reinforcement detailing in the joints is very crucial for the satisfactory structural performance of joints. Unsafe design and detailing within joint region jeopardizes the entire structure, even if other structural members conform to design requirements.

In reinforced concrete structures, detailing plays a vital role in how the structure behaves. Being a composite structure, the location of steel has significant influence on the stress distribution within the structure, and consequently on its behavior. A poorly designed detail in reinforced concrete can result in localized stress concentrations within the structure, which could result in failure. Such premature failure of structures occurs even where the structural members were designed to meet code requirements. Often, these failures occur in connection regions or corners (where there is an abrupt change in section), or in regions subjected to concentrated loading (like supports etc.). These regions are referred to as disturbed regions (or D-region). Sometimes however, poor detailing might not result in structural failures, but lead to a deterioration of the structure. Some typical deteriorations in reinforced concrete include formation of large cracks, spalling of concrete, corrosion of embedded steel etc. All these can be prevented or controlled with adequate detailing of the structure.

From a safety point of view it is important that a concrete structure, apart from necessary load capacity, also is able to show ductile behavior that allows redistribution of forces so that a local failure doesn’t lead to the total collapse of the structure. A structure’s ability to exhibit such behavior is highly dependent on the reinforcement detailing of the joint connections between its independent members.

Concrete structures should be detailed to satisfy safety, durability and serviceability requirements. For D-regions, EC2 section 9.9 clause-1 recommends designing D-regions with strut-and-tie models, and detailing them accordingly. Detailing of structural members and connections is a very important aspect of the design process. Though it is often viewed as preparing working drawing for a structure, it plays a crucial role in the performance on the final structure. It actually communicates the engineer's design to the contractor who oversees the construction on site. Where this communication is poor, the structure that is built may be different from what was assumed in design. Similarly, its behavior and capacity might differ from what was estimated in design. The importance of adequately designed joint details is often overlooked by the structural engineer. This is not surprising since in their professional training much time was spent learning how to design reinforced concrete beam and columns but very little time has been devoted to the design of corners and joints.

Various detailing systems for opening corner joints have been suggested from time to time. In this study, the efficiency of corner joint detailing is assessed by performing a nonlinear finite element analysis. The study focuses on the beam-column corner joints. The behavior of these regions was studied with the aim of understanding some key issues that would help achieve a satisfactory detail design.

1.2 Statement of the problem

Many structural failures that have occurred in history have been attributed to poor or wrong details. Calamitous incidents like the structural failure of Ronan point (in 1968), Hyatt Regency (in 1981), lignite bunker in Greece (2014) etc. could have been prevented if more attention had been paid to their structural detailing.

The principles of detailing and the structural behavior of simple structural members such as beams and columns are well established. On the other hand, the detailing, strength and behavior of corner joints, especially those subject to opening moments as in the case of cantilever retaining walls, bridge abutments, channels, rectangular liquid retaining structures and portal frames, have not been conclusively determined. It is assumed that the arrangements given are ''fully efficient'', i.e. they are capable of ensuring that the structural behavior implicit in the original assumptions can be realized.

In addition, few studies have been done on frame joints to define the joint detail, that could satisfy the requirement strength, limited cracking, ductility and simplicity of construction, and these details are different from one code to another.

1.3. Objective of the study

1.3.1 General objective

The recommended reinforcement detailing's must withstand loading at least as well as the connected members so that a safe and ductile structure is obtained. Hence, the main aim of this research project is to evaluate the detailing's given in Eurocode 2 for frame corners subjected to opening moments. A better understanding of the behavior of frame corners under loading to failure and of the structural response in the corner area is essential in order to check whether the above criterion is fulfilled.

1.3.2 Specific objectives

With their reinforcing bars detailed differently, corner joint behavior was studied in this thesis to provide answers to the following questions:

- How efficient are the considered joint layouts, and do they allow the structure to achieve its full capacity?
- Does the reinforcement layout affect the stress and strain distribution in the joint? How?
- How is failure likely to occur where these details are used?

1.4. Scope of the study

The scope of the present research work is limited to the following considerations:

I. Material property data and Strut and tie analysis of the corner frame is based on Eurocode 2.

II. Only static studies of the corner joints is considered, i.e. the corner was subjected to monotonic static loading.

III. Only corner beam-column joints are considered in the present study.

IV. The corner study was limited to frame corners of 90^0.

1.5. Outline of the Study

In total, this thesis is organized into five different chapters with the contents summarized as follows:

Chapter one, the introductory chapter, briefly describes the basics of detailing of frame corners. Furthermore, objectives of the thesis and the thesis outline are listed.

Chapter two, is an extensive literature study on the strut and tie methodology and on the behavior of corner joints. The first section discusses the concept of struts, ties and nodes, and how to dimension them. On the second section, different joint detailing are discussed based on experimental works available in literature conducted by several researchers including Nilsson (1973), Nabil et al. (2014) and Roshan et al. (2015). These experimental works give practical insight into the actual behavior of specimen with different detailing layouts.

In chapter three an analytical strut and tie design of a beam-column joint is undertaken. The geometric dimensions and capacity of the struts, nodes and tie are determined in this part of the thesis. Based on the ties, the reinforcement required is computed. The strut and tie method gives insight into the behavior of the joint when loaded.

Chapter four of the thesis introduces the subject of finite element method and the analysis of the beam column joint. Some aspects studied in this section include the influence of varying detail arrangements, and the role of stirrups and diagonal bars at re-entrant corners. Specific areas of interest include the joint efficiency of the structural details, their influence on stress and strain distribution within the joint, cracking behavior and eventual failure mode.

Finally, several conclusions are drawn and presented in Chapter five together with the discussion of possible future researches.

2. Literature review

2.1 Strut and Tie Model

2.1.1 Background on strut and tie modelling

A large number of Reinforced concrete structures present regions of discontinuity where beam theory is not suitable for the design of the reinforcement (Schlaich et al, 1987). Due to the presence of concentrated loads and changes in geometry, the stress and strain distributions within a structure are not always uniform. Schlaich et al (1987) proposed that the structure be categorized into one of two regions B or D depending on the strain distribution present. The respective B and D regions of a common structure are shown in Figure 2.1.

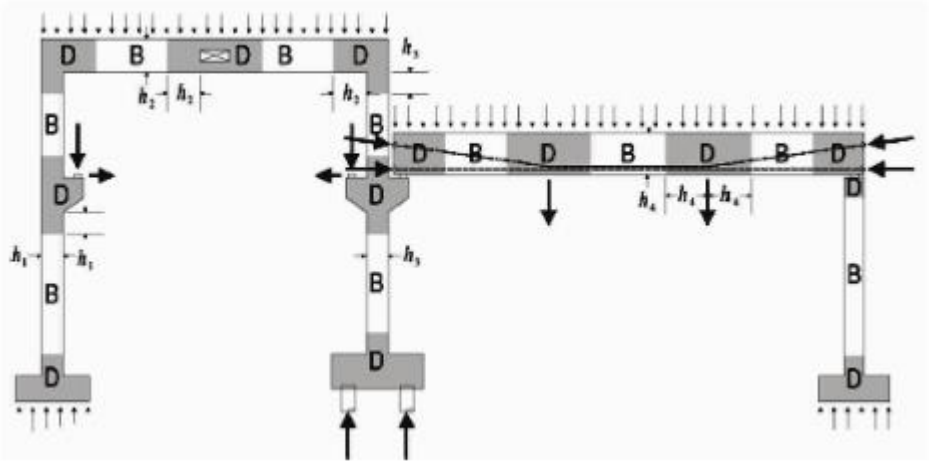

Figure 2. 1 Examples of division of B and D regions in common structures (Tjhin and Kuchma, 2002).

The structural components are divided into Beam regions (B-regions) and Disturbed regions (D-regions). In beam regions, it is reasonable to assume that there is a linear variation in strain over the depth of the section, whereas in Disturbed regions, there is a complex variation in strain, occurring near abrupt changes in geometry (geometrical discontinuities) or concentrated forces (statical discontinuities). The ordinary Bernoulli's theorem cannot be applied to such structures, as the plane sections don't remain plain after bending (Saeed et al, 2009). The principle of stress analysis or sectional analysis is not valid for such sections. Eurocode 2 (clause 6.5.1 and clause 9.9) recommends that such regions be designed with strut and tie models.

The extent of D-region spans approximately to one section depth according to St. Venant's principle as shown in Figure 2.2.

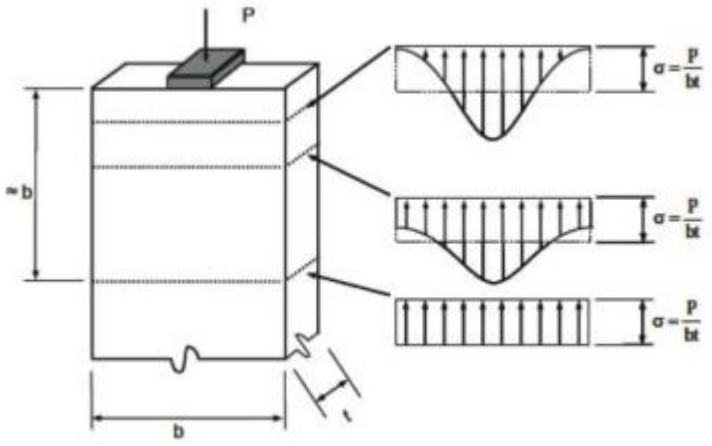

Figure 2. 2 Illustration of St. Venant's principle (FHWA, 2006).

The strut-and-tie method (STM) is emerging as a code worthy methodology for the design of all types of D-regions in structural concrete (Marti, 1985), (Schlaich, 1987), (Schlaich, 1991). The truss analogy and Strut and Tie Model (STM) have its root in the pioneering work of Ritter (1899) and Mörsch (1909), but the model has been extensively used for the analysis and design of deep beams, corbels, dapped ended beams, joints and beams having openings and discontinuities in the section during last one decade (Saeed et al,2009).

In STM, a load-resisting truss is idealized to carry the forces through the D-region to its supports. The shape of the load resisting truss and its selection depends on the experience of the designer, who is free to choose the shape of the load-resisting truss with only limited guidance and constraints. The structure is assumed to be sufficiently ductile so that the load is supported in the same fashion as envisioned by the designer and no part of the truss is over stressed. The compression members of the Truss are called Struts, which resist the compression forces and the struts capacities are determined on the basis of equations proposed by Eurocode 2. These struts are assumed as prismatic, bottle shaped or fan shaped. The tensile members of the truss are called ties, which are reinforced with steel bars. The joints of truss are called "Nodes" (Tjen and Kuchma, 2002).

For the design of complex D-regions, the designer must exercise greater care in the selection of an appropriate idealized truss, application of STM code provisions, the plasticity assumption, and the performance of the structure under service loads.

2.1.2 Design steps of disturbed regions by strut and tie model (STM)

Brown et al. (2008) have proposed the following steps for the design of disturbed region by STM. It is shown in a flowchart in Figure 2.3.

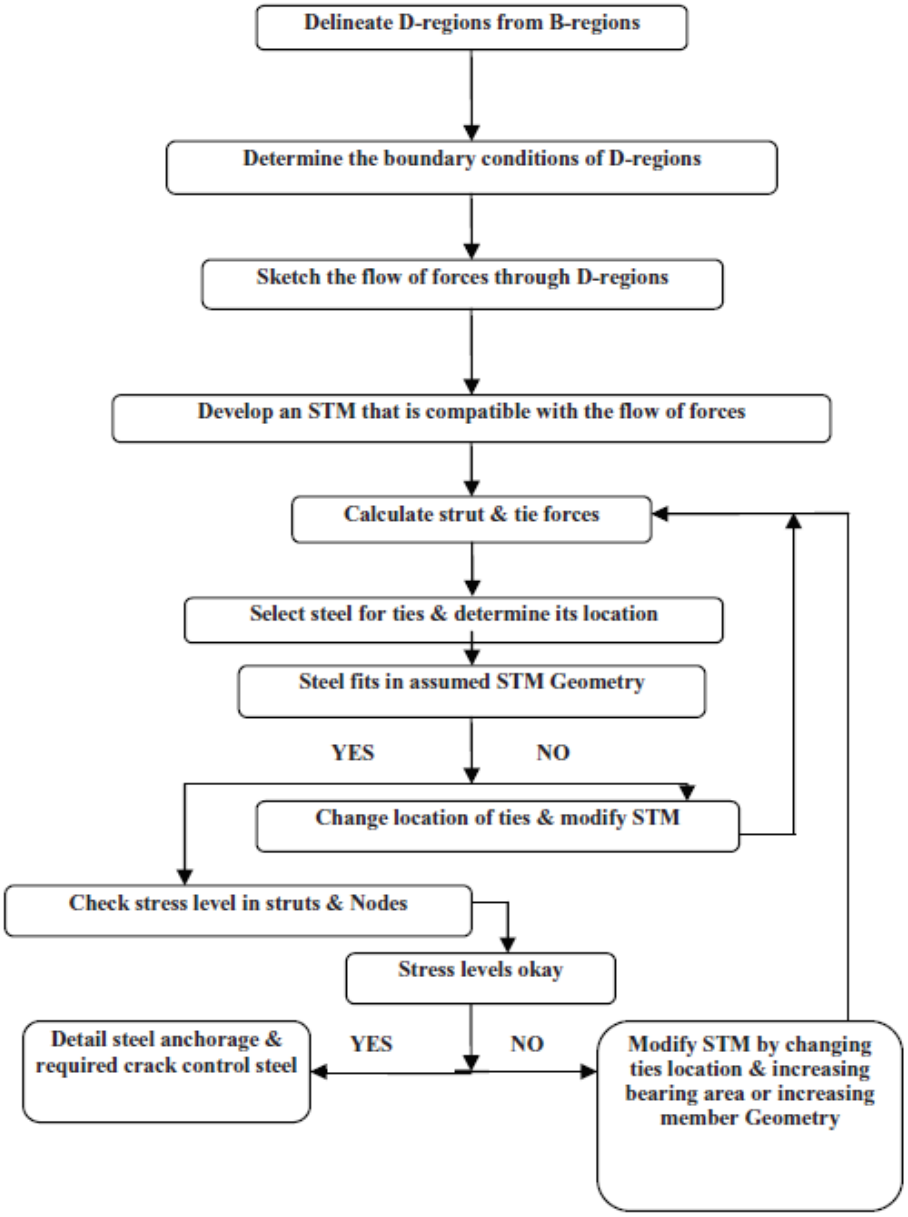

Figure 2. 3 Flowchart illustrating STM steps. (Brown et al. 2008).

2.1.3 Components of strut and tie model

A typical strut and tie model comprises of compression struts, tensile ties and nodal regions. In this section, each of these components would be discussed, and details would be given on how they are dimensioned, and how the strengths are determined for design purposes.

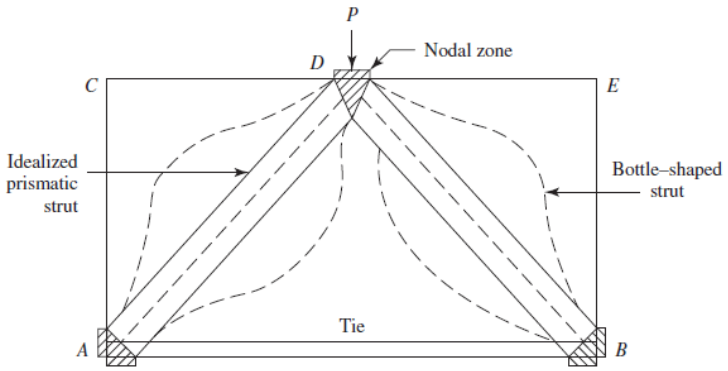

Figure 2. 4 Strut and tie model (for illustration)

2.1.3.1 Struts

This is an internal compressive member in a strut and tie model that represents the compressive stress field within the concrete section. The centerline of the strut is oriented along the principal compressive stress trajectory in the un-cracked stage. The strut can be of unreinforced or reinforced concrete. From Figure 2.4, the members AD and DB are the struts. The shape of struts could be prismatic, bottle-shaped or fan shaped. The prismatic strut (as in Figure 2.4) is parallel between two nodes, and it is assumed that the bearing area does not change. The bottle-shaped strut is wider along the length (than at the ends) as stresses are allowed to spread in the section. The dashed lines in Figure 2.4 demonstrate spreading of the stress along the strut length. In a bid to maintain equilibrium, this spreading of stress gives rise to transverse tensile stresses that could result in splitting cracks as illustrated in Figure 2.5. After cracking, the strut may fail if transverse reinforcement is not provided. Where provided, transverse reinforcement would control longitudinal splitting cracks, and the failure mode would then be governed by crushing. The likelihood of transverse splitting makes the bottle shaped strut to be inherently weaker than a prismatic strut. For the fan-shaped strut, an array of struts at different angular orientation originates from, or meet at a single node.

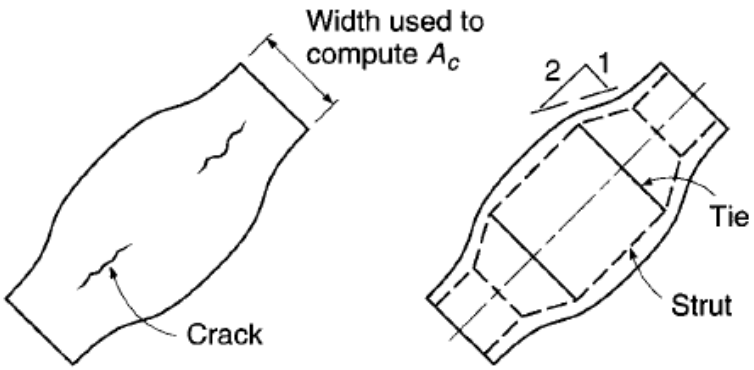

Figure 2. 5 Cracks in bottle-shaped strut from transverse tensile stress (Nilson, Darwin and Dolan, 2004)

Eurocode 2 (EC2) gives guidance on estimating the transverse tensile forces in a bottle-shaped strut. There are two possibilities depending on whether the strut is partially disturbed (i.e. partial discontinuity in Figure 2.6a) or fully disturbed (i.e. full discontinuity in Figure 2.6b). Partial discontinuity occurs when the width of the strut is less than half of its height i.e. ($b \leq H/2$ in Figure 2.6a). In this case, a B-region can occur between two D regions in the struts. The transverse tensile force in the strut can be obtained from expression 6.58 of EC2 shown below:

$$T = \frac{1}{4} \cdot \frac{b-a}{b} \cdot F \qquad (2.1)$$

For a fully distributed strut, the entire section is a D-region, and can also be obtained from expression 6.59 of EC2 given thus:

$$T = \frac{1}{4} \cdot \left(1 - 0.7\frac{a}{h}\right) \cdot F \qquad (2.2)$$

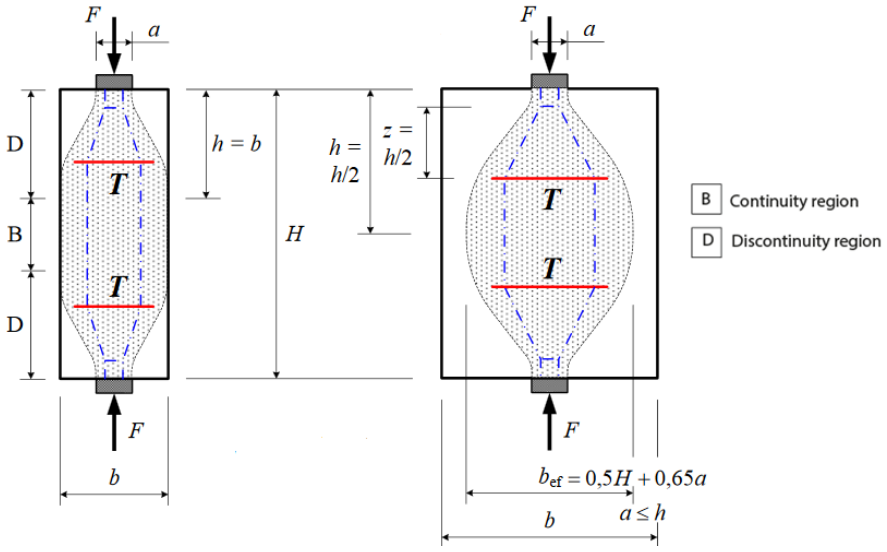

a) b)

Figure 2. 6 Partial discontinuity (a) and full discontinuity (b) regions arising from compression stress (Westberg, 2010)

The capacity of struts (F_{cu}) can be estimated with the expression:

$$F_{cu} = A_c \cdot \sigma_{Rd,\max} \qquad (2.3)$$

Where A_c is the effective cross sectional area of the strut and $\sigma_{Rd,\ \max}$ is the effective design strength.

The design strength of concrete struts is influenced by the multi-axial stress state and the presence of cracks and/or reinforcement. If the concrete is subjected to uniaxial compression , as shown in Figure 2.7, Eurocode 2 clause 6.5.2(1) allows the design strength of the concrete to be used.

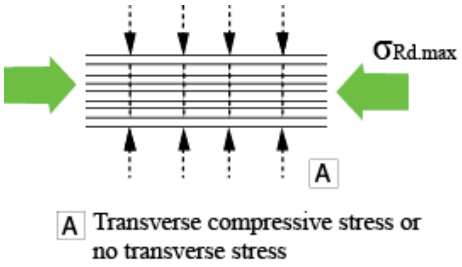

Figure 2. 7 Design strength of concrete strut (no transverse tension), EC2

$$\sigma_{Rd,\,max} = f_{cd}, \text{ where } f_{cd} = \alpha_{cc} f_{ck} / \gamma_c \qquad (2.4)$$

Where f_{ck} is the characteristic cylindrical strength at 28 days, α_{cc} is a coefficient that takes load duration effect into account with a value between 0.8 and 1.0. A value of 0.85 is used in this work. γ_c is the material partial safety factor for concrete taken as 1.5 from table 2.1 N of EC2.

Where axial compression of the strut is accompanied by transverse tension, as shown in Figure 2.8, a lower design strength is used express as:

$$\sigma_{Rd,\,max} = 0.6 \cdot \left[1 - \frac{f_{ck}}{250}\right] \cdot f_{cd} \qquad (2.5)$$

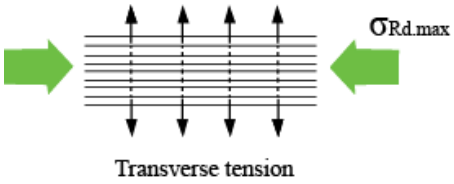

Figure 2. 8 Concrete strut with transverse tension

2.1.3.2 Ties

These are tension member in the strut and tie model. The tie consists of the reinforcement, and a portion of concrete concentric around the diameter of the tie. The concrete portion defines the effective width of the tie. This concrete however does not contribute to the tensile strength of the tie. It nevertheless adds the stiffness by the tension stiffening effect, and thus helps to control deformations. The steel bars used as ties could be in one layer or smeared in several layers over the length of the tensile zone. The centroid and direction should however be the same as that of the tie in the model. When distributed in several layers across the tensile zone, better crack distribution would be achieved. The capacity (F_{tu}) of ties is expressed thus:

$$F_{tu} = f_{yd}A_s + \Delta f_p A_p \quad (2.6)$$

Where the design strength steel $f_{yd}=f_{yk}/\gamma_s$

The ties need to be properly anchored into the nodes so that the tensile strength of the tie can be fully developed, and to prevent premature tie failure.

2.1.3.3 Nodes

Nodes are the points where the forces in struts and ties intersect and balance within the strut-and-tie model. According to the model, forces converge, and they are transferred or redirected at that point. A node is essentially a defined volume of concrete, acted upon by different forces. Conceptually, MacGregor and Wight (2005) note that they are idealized as pinned joints where three or more forces meet, and are in equilibrium i.e.

$$\sum F_x = 0 \qquad \sum F_y = 0 \qquad \text{and} \qquad \sum M = 0$$

The $\sum M = 0$ condition requires the line of action of all active forces to pass a common point. Schlaich et al. (1987) described the concept of nodes as a "simplified idealization of reality". The forces that meet at a node are in reality stress fields represented by struts, reinforcing bars which are anchored around the nodal region, and externally applied concentrated loads or support reactions.

Based on the combination of compressive (C) and tensile (T) forces acting on the nodal zone, nodes can be classified into three basic types as illustrated in Figure 2.9.

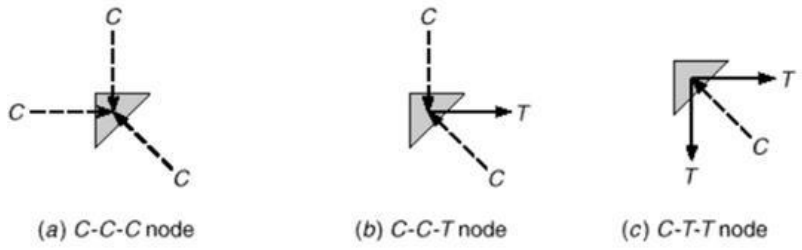

Figure 2. 9 Classification of nodes

Section 6.5.4 of EC2 gives guidance for determining the maximum stress ($\sigma_{Rd,max}$) which can be applied at the edges of the node. The general expression is presented as:

$$\sigma_{Rd,\max} = k_i \cdot \left[1 - \frac{f_{ck}}{250}\right] \cdot f_{cd} \quad (2.7)$$

Where

K_1=1.0 for CCC node

K_2=0.85 for CCT node

K_3=0.75 for CTT node

Where $f_{cd}=\alpha_{cc} f_{ck}/\gamma_c$

From the above expression, it should be observed that the nodal strength is lower than the typical design value once there is tension. When a tensile tie is anchored in the nodal zone, there is likely to be incompatibility between tensile strains in the reinforcing steel and compressive strain of the node.

2.1.3.4 Dimensioning strut and tie components

The nodes, struts and ties of the idealized truss in a strut-and-tie model usually have theoretical dimensions. These dimensions are its width and thickness. The thickness is often taken as equal to the member thickness. The effective width of a strut and the nodal zone are often the unknowns in strut and tie design. They are determined based on the forces acting on the node, and the dimensions of the adjoining element. The product of the effective width and thickness is called the bearing area.

A useful concept in dimensioning struts and nodes is that of "hydrostatic nodes". A nodal zone is "hydrostatic" if the stress on each face of the node is the same. The nodes are dimensioned in such a way that the ratio of their width is proportional to the compressive stress acting on that face. However, achieving hydrostatic nodes for STM geometric configurations is almost impossible and usually impractical. For this reason, STMs with non-hydrostatic nodes are more common. For non-hydrostatic nodes, Schlaich et al. (1987) suggest that the ratio of maximum stress on the face of a node to the minimum stress should be less than 2. The states of stress in hydrostatic and non-hydrostatic nodes are shown in Figure 2.10.

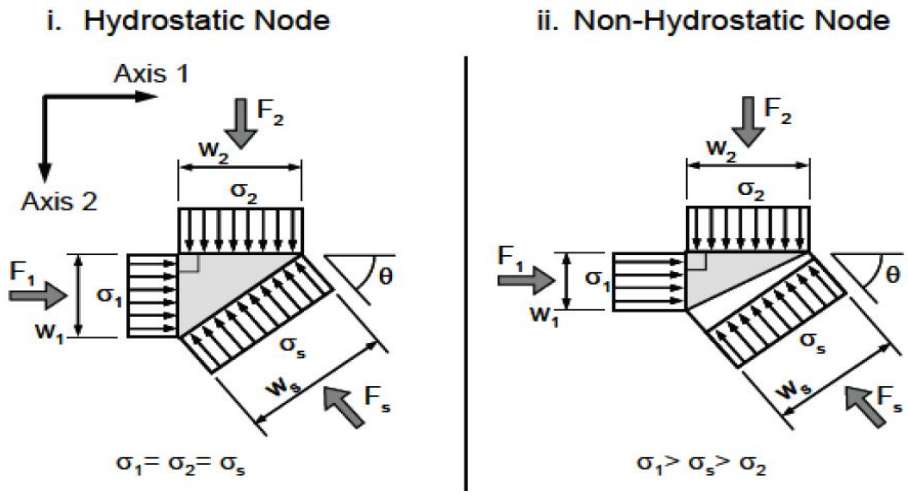

Figure 2. 10 Hydrostatic and Non-Hydrostatic nodes

2.2. Reinforcement detailing in frame corners

2.2.1 Introduction

Reinforcement detailing at corners plays a primary role in influencing the structural behavior of the joint, particularly in the case of opening corner joints. This is for instance the case of corner regions of frames, stairs, cut-and-cover tunnels, retaining walls, silos or folded structures as shown in Figure 2.11. The behavior of nodal regions is highly dependent on the reinforcement arrangement which ensures the transfer of inner forces and typically governs the strength and deformation capacity of the structure (Foster et al, 1996). From a safety point of view it is important that such structures, apart from necessary load capacity, also exhibit ductile behavior so that a local failure does not lead to total collapse of the structure. A structure's ability to meet this requirement is highly dependent on the reinforcement detailing used in the joint connections. The positioning of the reinforcing steel in the adjoining members is often obvious; however, this is not the case in corner joints. Compared with the former, the detailing of corners in reinforced concrete frame structures represents a relatively untouched field. Despite important contributions made by, Nilsson (1973), Mayfield et al. (1972), and Stroband and Kolpa (1981, 1983), for every test made on a corner joint several hundred tests to check the bending and shear capacity of beams have been carried out.

Beam-Column joints in a reinforced concrete moment resisting frame are crucial zones for transfer of loads effectively between the connecting elements in the structure. It has been observed that during earthquakes, Corner Joints are under heavy distress due to shear in the joints which results in the collapse of the structure. The previous studies have confirmed that corner joints subjected to opening moments are more critically influenced by the detailing of reinforcement than those subjected to closing moments. There is sudden change in geometry and complexity of stress distribution at joints of reinforced concrete framed structures which makes these joints critical. Design of Beam-Column joints in RC framed structures was generally based to satisfy anchorage requirements initially. But nowadays it has been found out that behaviour of joints depends on a number of factors such as Geometry of structure, reinforcement detailing, strength of concrete, Reinforcement strength, type of loading, etc.

Ideally, a joint should resist a moment at least as large as the calculated failure moment of the members framing into it, and ensure ductile behavior in the ultimate limit state. Park and Paulay (1975) and Nilsson (1973) summarized the requirements for a corner subjected to bending as:

- the joint shall be able to withstand a moment of at least the same magnitude as those on the adjoining sections;

- for joints which do not satisfy the above design criterion, the ductility shall be sufficient to prevent brittle failure so that redistribution of forces in the structure will be possible;
- crack widths at corners under service load shall be limited to an acceptable magnitude;
- The reinforcement shall be easy to fabricate and position; the risk of incorrect detailing is significantly decreased when a simplified detailing is used.

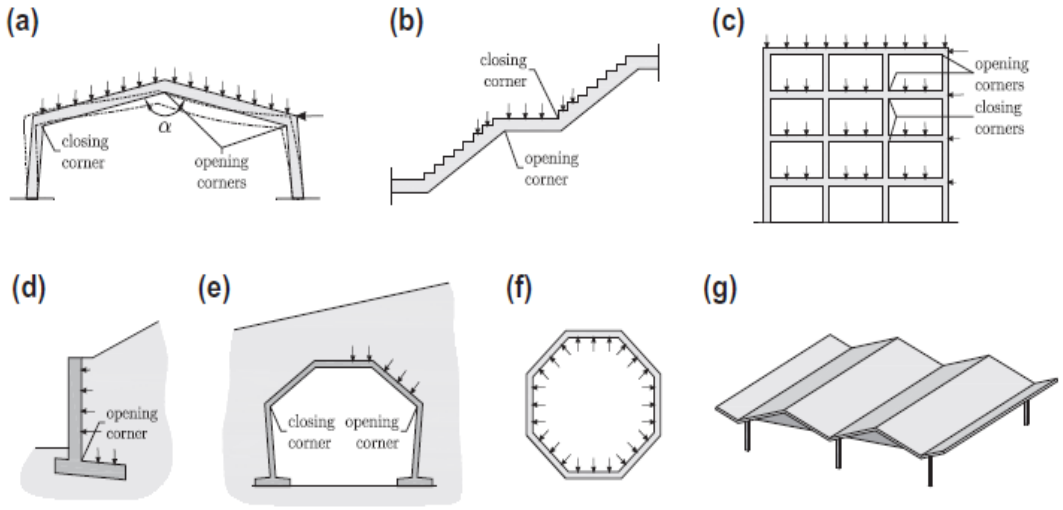

Figure 2. 11 structures subjected to opening and closing moments (Campana et al. 2013)

2.2.2 Failure modes of concrete joints

In opening corners, failure of the joint may be caused for various reasons depending on the amount and layout of reinforcement. Some of the reasons are: a) splitting failure of concrete or anchorage failure of the reinforcement anchored in the joint, b) excessive cracking starting from the inner part of the reentrant corner due to tensile stresses ([σ_x] in Figure 2.12), c) diagonal tension cracking due to tensile stresses parallel to the corner diagonal ([σ_y] in Figure 2.12), d) failure of a member converging to the joint due to shear or bending and e) failure due to yielding of reinforcement.

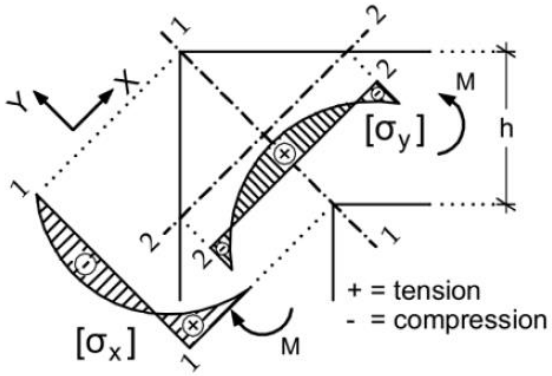

Figure 2. 12 Stresses σ_x and σ_y in a right-angled corner subjected to opening moment (Moretti, 2014)

Cracks initiating from the reentrant corner are of bending type and not critical since they are restrained by the adjacent compressive stresses σ_x. Diagonal tension cracks caused by stresses σ_y may lead to brittle splitting failure of the joint if the diagonal crack is not controlled by reinforcement. Diagonal tension cracking failure occurs in the core of corner joints due to the presence of quite large shear forces acting concurrently with the applied opening moments. This mode of failure is illustrated in Figure 2.13.

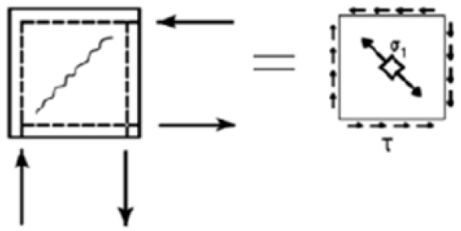

Figure 2. 13 Diagonal tensile failure illustration (Hsu and Mo, 2010)

The flexural action generated by the applied moment acts against an idealized free body (represented by the square corner in Figure 2.13) subjected to uniform shear. This combined action of shear and flexural stresses results in the tensile principal stress σ_1 inclined at an angle in Figure 2.13. Diagonal tensile cracking occurs in a direction perpendicular to σ_1 once the transverse tensile stresses exceed the concrete tensile strength. Ideally, reinforcement representing tensile ties should be oriented in the direction of the principal stress (σ_1) if they are to be effective in controlling the crack. Diagonal tensile cracking failure is a rather brittle failure, and could lead to premature failure of the structure. Diagonal tension cracks should be taken into consideration when detailing any joint type subjected to opening moment.

2.2.3 Definition of corner efficiency

As stated in Section 2.2.1, the strength of a corner shall ideally be at least as large as that of its adjoining members. In what degree this requirement is fulfilled, is normally expressed as corner efficiency, and in the following sections this term will also be frequently used in the discussion of different reinforcement detailing of frame corners.

The corner efficiency in literature is defined as the ratio between the moment capacity obtained in tests, independent of what final failure mode is obtained, to the theoretically estimated moment capacity of the members (weakest member used) making up the corner. (Johansson, 2000)

$$\text{corner efficiency} = \frac{\text{moment capacity of frame corner obtained in tests}}{\text{theoretical moment capacity of adjoining member}}$$

In this study, it is defined as the ratio between the moment capacity obtained in the VecTor2

simulation, to the theoretically estimated moment capacity of the members as calculated in section 3.3.

The corner efficiency must be greater than or at least equal to one (or 100%, in percentage form) in order for the joint to be as strong as the weaker cross section framing into it.

2.2.4 Requirements in Eurocode 2

Eurocode 2, Annex J.2.3 gives recommendation concerning detailing of concrete frame corners subjected to opening moment. In Figure 2.14 frame corners subjected to moderate opening moment are shown, which also can be found in Figure EC2 J.3.

a) *b)*

Figure 2. 14 Frame corner with moderate opening moment (Eurocode 2)

The tensile reinforcement amount that is recommended in Eurocode 2 is expressed according to Equation (2.8)

$$\rho = \frac{A_s}{b \cdot d} \leq 2\% \qquad (2.8)$$

A_s area of the tensile reinforcement

b width of the concrete cross-section

d effective depth of the cross-section.

In Figure EC2 J.4 recommendation regarding detailing of concrete frame corners subjected to large opening moment are illustrated, which also are repeated in Figure 2.15.

a) *b)*

Figure 2. 15 Frame corner with large opening moment (Eurocode 2)

The tensile reinforcement amount that is recommended in Eurocode 2 is expressed according to Equation (2.9)

$$\rho = \frac{A_s}{b \cdot d} > 2\% \qquad (2.9)$$

2.2.5 Behavior of different corner joint details

A number of detailing arrangements for opening corners have been proposed from time to time by various researchers which are discussed here after.

Several reinforcement layouts were cast into the 90° angled specimen by Nilsson's (1973) and loaded to failure. The behavior of specimens with these layout and their respective joint efficiencies is discussed here below.

In the traditional reinforcement layout test, where tensile bars are bent 90^0 (U20, U21 and U22 in Figure 2.16) the corner joint failed with large deflections measured, there were no signs of damage on the adjacent connected members as failure occurred at a moment around one-third of the calculated moment (32% joint efficiency). It was caused by diagonal tension cracking failure.

Like the result of the traditional layout, Hairpin reinforcement layout (U14, U15 and U16 in Figure 2.16) also failed due to diagonal tension cracking. However, it needed larger applied loads to failure, thus giving a higher joint efficiency of 68%. Diagonal cracking was forced to the corner of the hairpin (in comparison with the traditional layout) thus resulting in the larger capacity of this joint.

For Reinforcement with loops the concrete portion outside the loop (U11, U12 and U13 in Figure 2.16) was detached .Compared with the earlier two reinforcement details discussed, this gave a higher joint efficiency of 77%.

Using inclined stirrups (U28 in Figure 2.16), the layout gave a joint efficiency of 79% thus significantly increasing capacity when compared to the case without stirrups. The use of stirrups strengthened and improved performance of the corner joint (Nilsson, 1973). At failure, though neither the main reinforcement nor the diagonal stirrups yielded, diagonal cracks still occurred, in addition to the cracks at re-entrant corner.

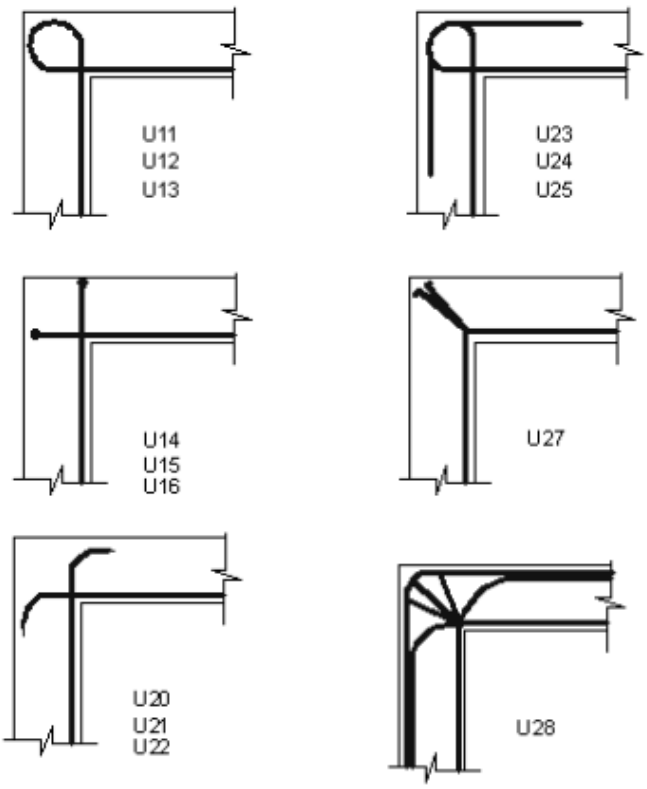

Figure 2. 16 Test Specimens of Nilsson (1973)

Satisfactory results were obtained by using loop reinforcement with diagonal bar at re-entrant corner (refer Figure 2.17): that detail was improved by adding a diagonal around the inner corner to control the cracks that normally initiate at the re- entrant corner, thus preventing separation of the inner corner.

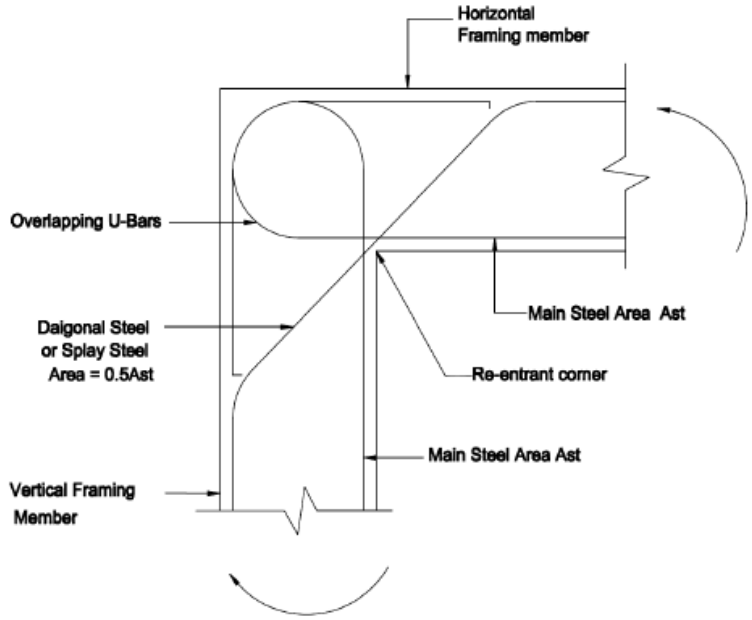

Figure 2. 17 Recommended detail by Nilsson (1973)

Nabil et al. (2014) performed an experimental study on eleven corner joints subjected to opening moments to study the joint efficiencies, crack and deformation pattern, effect of stirrups, joint size and comparison with closing joints. The behavior and crack pattern are comparable to that from Nilsson's (1973) work thus with diagonal tension playing a governing role in many of the specimen. The use of looped reinforcement arrangement of the main tension reinforcement gave the best result. Adding a diagonal bar at the re-entrant corner improved the result even further for looped details. However, the use of diagonal bar did not help significantly for details susceptible to diagonal tension cracking. However, where stirrups were used for such details, and placed in a fan-shaped arrangement (i.e. smearing outwards from the inner corner to the outer, thus crossing the crack trajectory) improvements were made and the joint thus reached full capacity. This is however contrary to the result Nilsson (1973) obtained with stirrups, as the stirrups gave marginal benefit in that case, without reaching 100% efficiency. More experiments from other authors could clarify this discrepancy.

Campana et al. (2013) performed experiment on sixteen corner specimen (most of which were of 125° angle). The result were also comparable to those obtained by Nilsson (1973). On the comparison of the layout of the main flexural reinforcement, the looped detail gave the best result though below 100% efficiency. It was improved by the addition of diagonal bar at the re-entrant corner. The use of stirrups in the corner joints also increased the capacity of the traditional layout (which is susceptible to diagonal tension failure) with over 100% efficiency achieved. Though Nilsson's (1973) study differed on this issue of transverse stirrup reinforcement, the effectiveness of stirrups has however been confirmed by Campana et al. (2013), Nabil et al. (2014), Park and Paulay (1975) and Lao and Hsu (2010). It is also one of the two recommended details for opening corner in EC2 Annex J.2.3. In all these cases, the use of stirrup is combined with a diagonal bar at the re- entrant corner. In his work, Nilsson only used inclined stirrups without the diagonal bar at the re-entrant corner. Much higher joint efficiency could have been achieved otherwise.

The results from the tests summarized in Johansson (2000) indicate that the solution of Type 1 and Type 2 (shown in Figure 2.18) show poor performance. However, Campana et al. (2013) chose to investigate these details further to see if the corner efficiency could be effectively improved by adding radial stirrups to the solution of Type 1. The result showed that the behavior was effectively improved from an efficiency of 36% to 85%. However, Johansson (2000) argues that the corner efficiency is not improved by adding radial stirrups.

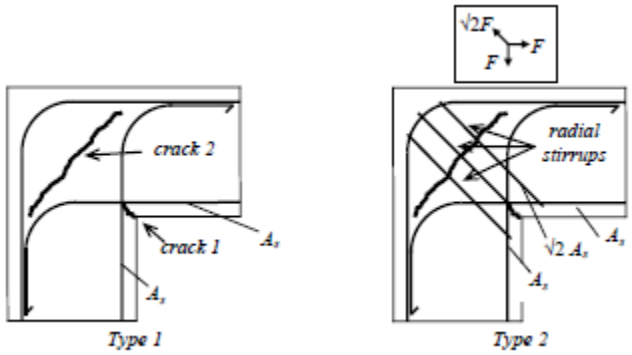

Figure 2. 18 Type 1 and Type 2 detailing tested by Johansson (2000)

The Indian standard has recommended detailing for opening corners as shown in Figure 2.19. Depending upon the main tension steel content (less than 1% or greater than 1%), three different types of detailing arrangements have been proposed for reinforcing opening corners.

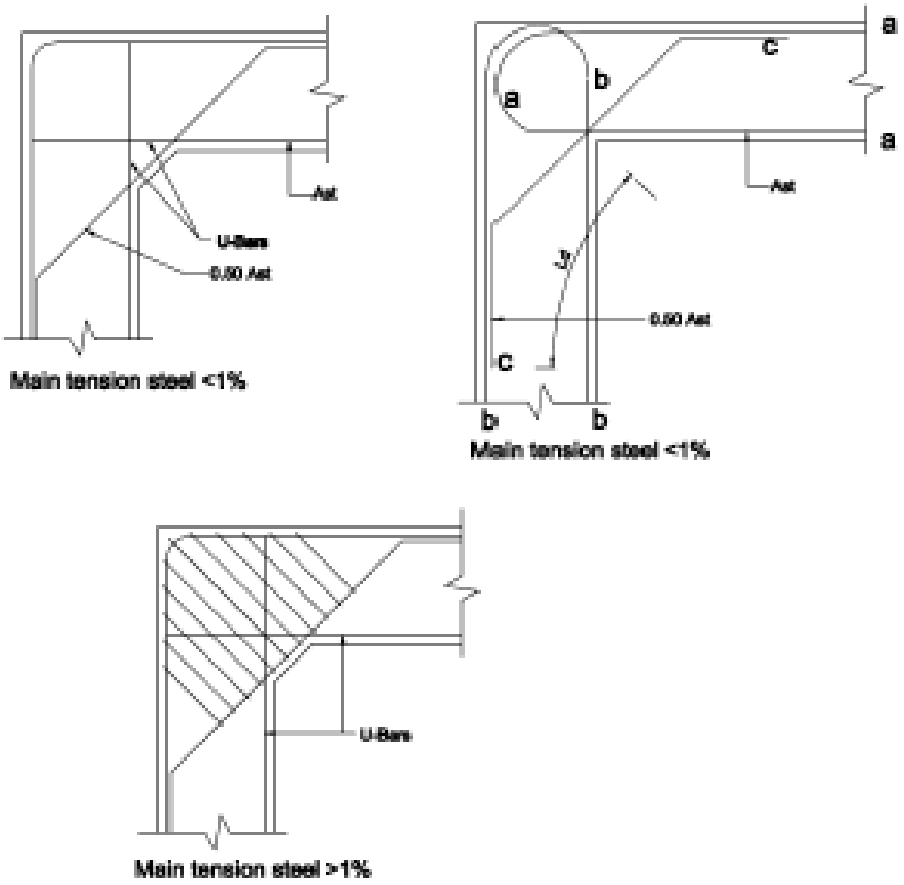

Figure 2. 19 Detailing of Opening Corners Recommended by Bureau of Indian Standards (1999)

ACI 315-92 has recommended detailing for wall intersections and corners (Figure 2.20).

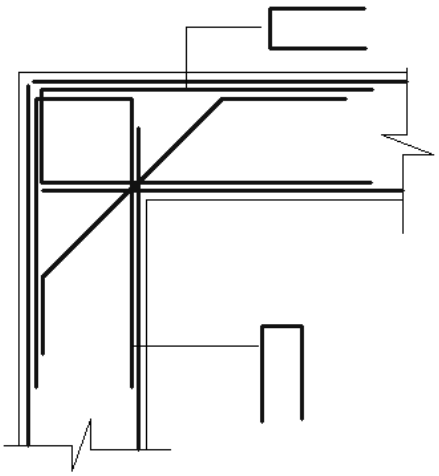

Figure 2. 20 Detailing of Wall Intersections and Corners Recommended by ACI 315-92.

Kaushik and Singh (2003) conducted an experimental study to evaluate the structural behavior of opening corners. Four different detailing systems were investigated. The parameters of investigation were: strength measured in terms of joint efficiency, ductility, crack control, and ease of reinforcement layout and fabrication facilitating effective placement of concrete in the member. It has been found that none of the detailing systems investigated satisfied all the four parameters. A substantial increase in post-cracking tensile strength, ductility and crack control can be achieved by adding steel fibers to the concrete.

V.N. Dhar and Dr. P K Singh, (2004) investigated the effect of chamfer as well as reinforcement detailing on strength and behavior of opening corners. It was observed that cracking in the corner region reduced with increase in chamfer. Failure load and joint efficiency increased with increase in chamfer. Inclined bar at re-entrant corner gets more lever arm and loop steel gets additional anchorage due to presence of chamfer. They also studied the stress variation in joint by linear finite element analysis and concluded that overall stress level in the corner decreased with increase of chamfer size. It was suggested that a chamfer of size equal to the thickness of framing member may be used in corner joints subjected to opening moments.

Park and Mosalam (2012) carried out an experimental investigation of full-scale RC corner beam-column joints without transverse reinforcement in the joint region. The experimental study considered two design parameters: joint aspect ratio and beam longitudinal reinforcement ratio. Four corner beam-column joint specimens were constructed with transverse beams and floor slabs and tested under quasi-static cyclic loading. The specimens experienced joint shear failure without beam hinging mechanism as a result of the absence of transverse reinforcement in the joint region.

After the appearance of extensive cracks in lignite storage bunkers at a power generating station in Greece, Moretti et al. (2014) undertook an experimental study in order to clarify the influence

of the detailing of reinforcement to the pattern of cracking. The detailing of reinforcement in the joints was considered to be one of the causes of the damage observed. Specimens in natural scale (1:1) were constructed and subjected to repeated opening moment, so as to simulate the loading conditions of the real structure while being filled and emptied. It was stated that anchoring of the tensile reinforcement by a hook of 180 or 225 degrees resulted in reduction of overall cracking.

Improvement (in terms of strength and behavior) of a corner joint subjected to an opening moment using steel fibers was studied by Abdul-wahab and Al-Roubai (1998). Twenty-three corner specimen with varying amount of steel fibers (maximum was 2% by volume). Only two reinforcement details were used i.e. the looped layout (without diagonal at re-entrant corner) and looped layout (with diagonal at re-entrant corner). The corner angles were also varied from 60° to 150°. Addition of steel fibers had noticeable impact on the failure mode. Without the fibers, diagonal tension failure governed in the samples. Diagonal tension failure also governed for all corner specimens with 0.5% fiber content, and most of the 1.0% fiber content. However, for samples with 1.5% and 2.0% steel fibers in the joint, the failure mode became yielding of reinforcement at the adjoining member's away from the joint. Similarly, Bansal et al. (2008) stated substantial increase in post-cracking tensile strength, ductility and crack control can be achieved by adding steel fibers to the concrete. The investigations indicated that in the specimen, there is a 30%-35% gain in efficiency with increase in volume fraction up to a certain limit beyond which there is a drop in mix workability and joint efficiency.

2.2.5.1. Impact of reinforcement ratio on corner joint efficiency

Depending on the concrete and steel properties used in the experiments, Nilsson (1973) calculated a maximum reinforcement ratio of 0.3% in his work. This means that brittle failure would not occur for the specimen (used for that work) if the main reinforcement ratio was less than or equal to 0.3%. The steel would yield and the joint would be ductile. However, using such a low reinforcement ratio would only work for rather small forces. For the load types typically encountered in practice, such a low reinforcement ratio would yield resulting in large cracks and deformations, and subsequent failure. The reinforcement ratio for most structures in practice ranges from 0.5% to 2%.

In the test of Mayfield (1973), the full moment capacity was achieved when reinforcement was held to 0.75%. The same conclusion was set by Nilsson (1973). Tests by swann (1969) on steel joints with steel ratios equal to 3%, indicated failure at less than 80% of the design strength as discussed also by Park and Paulay (1975).

In view of the fact that diagonal tensile stresses occurs mainly due to large shear forces in the corner joint. As the force in the reinforcement increases, the shearing stresses with the joint also increases, thus resulting in higher splitting tensile stresses. For this reason, Park and Paulay (1975) and Kaliluthin, Kothandaraman and Suhail-Ahamed (2014) recommend increasing shear (transverse) reinforcement for medium to highly reinforced sections. In addition to the surrounding concrete, it would provide confinement to the concrete. Though the concrete could still crack, the concrete within the cracks would still contribute to performance of the joint via tension stiffening effect, hence reduce deformation in the section.

The importance of the detailing on the behavior of opening corners in reinforced concrete structures has been often pointed out in the past and some relevant research has been conducted, as discussed previously. But most experimental research done by researchers such as Al-Khafaji (2011), Roshan (2015), Campana (2013) and others, used a tensile reinforcement ratio of 0.7%-0.8%. Hence they were unable to account the effect of reinforcement ratio in their research work. And the correlation of reinforcement ratio and corner efficiencies were neglected. In addition, the reinforcement detailing's shown on Figure 2.14b and 2.15b have not been studied experimentally in the past and are drawn directly from the strut and tie model. Hence, in this thesis their behavior is studied thoroughly. The effect of reinforcement ratio is also studied in order to study the influence it has on corner efficiencies.

The effect of different detailing systems has been investigated in the laboratory but surprisingly, numerical modelling has received lesser attention. Hence, this thesis aims to supplement the experimental analysis by conducting a nonlinear finite element analysis.

3. Analytical Design using strut-and-tie model

For this study, a portal frame was used to investigate the significance of structural details in a structure. As discussed in the previous chapter, the beam-column joint of a portal frame is a disturbed region (D-region). Accordingly, in this section, strut-and-tie methodology is used to analyze force transfer in the D-region of the beam-column joint. Two strut and tie schemes, referred to 'scheme-1' and 'scheme-2', are used by applying 15kNm and 19.2kNm moments respectively. The design loads required for the strut and tie modeling are the boundary stresses caused by these bending moments. Figure 3.1 shows the D-region of the beam-column joint, with an opening bending moments, M_{ED}, acting on its boundaries.

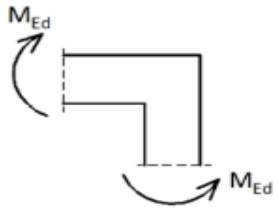

Figure 3. 1 Sample D-region of a corner joint

3.1 Input data for frame corners

The corners taken for analysis have common properties, which are listed below.

Concrete:

C30/37

Characteristic compressive strength: f_{ck}=30MPa,

Design compressive strength: f_{cd}[1] =f_{ck}/γ_c=30/1.5MPa= 20 MPa

Steel:

S-400

Characteristic yield strength f_{yk}= 400 MPa

Design yield strength: f_{yd}= f_{yk}/γ_s=400/1.15MPa= 347.82 MPa

Dimensions of members h= 200mm, b (out of plane) =160mm

3.2 Strut and tie scheme

As recommended in the Eurocode, scheme-1 and scheme-2 are proposed for joints under moderate opening moments and large opening moments respectively. They are presented in the Figure 3.2 below.

[1] f_{cd} is 16.67MPa when the characteristic strength is divided by the partial safety factor for concrete. In a strut and tie model, this value is further reduced by a factor α_{cc} depending on the node type. Refer section 2.1.3.3.

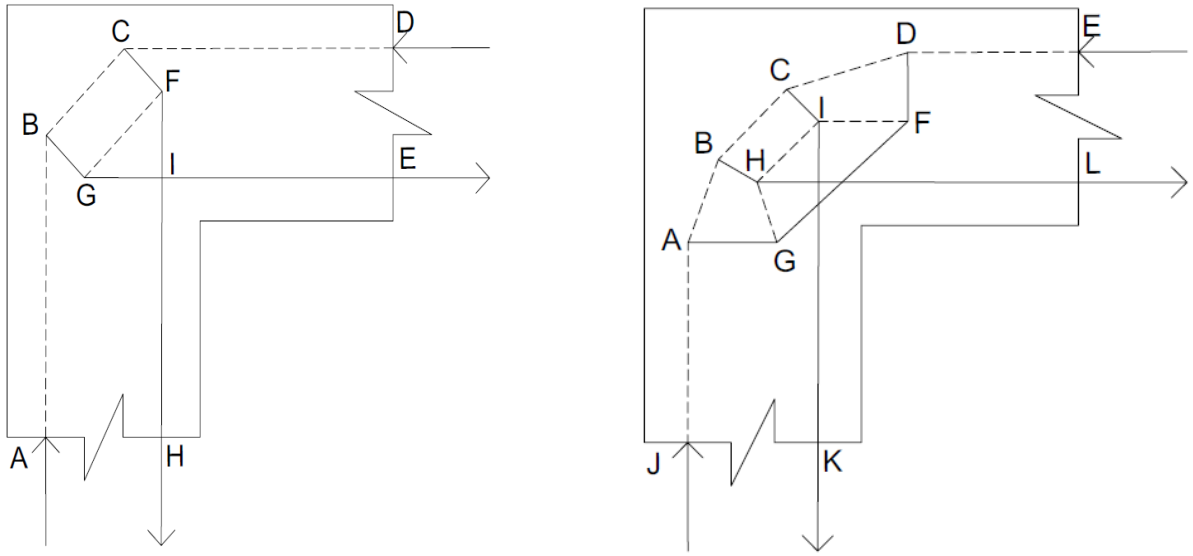

a) scheme 1 b) scheme 2

- - - - - - - Dashed lines represent struts
——— Solid lines represent ties

Figure 3. 2 proposed strut and tie models

For scheme-1,(strut and tie model for corners subjected to moderate opening moments), both corners are loaded with an opening bending moment of 15 kNm modeled as a pair of forces of magnitude 125kN and the distance between the forces is 120mm.

For scheme-2, (strut and tie model for corners subjected to large opening moments) both corners are loaded with an opening bending moment of 19.2 kNm modeled as a pair of forces of magnitude 160kN and the distance between the forces is 120mm.

3.2.1 Strut and tie analysis of the joint, scheme-1

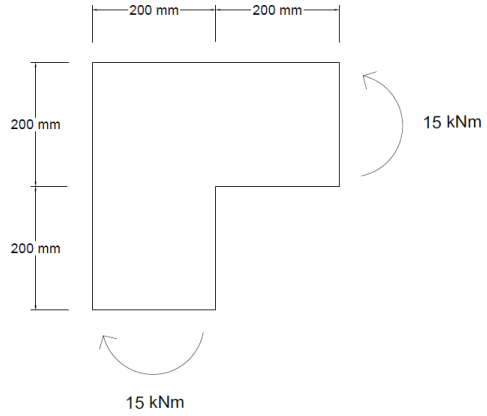

Figure 3. 3 Delineated D-region of a beam-column joint (scheme-1)

In this section, the delineated D-region of Figure 3.3 was analyzed using the strut-and-tie method. The flow of forces in the corner joint is estimated to understand stress transfer in the joint, and

to guide the detailing of reinforcement for the joint. The sequence of steps to be followed in strut and tie design was illustrated in Figure 2.3 and is followed in this section.

Force flow in the D-region

The bending moments acting on the section caused bending stresses at the boundaries of the D-region. The corner joint is subjected to 15kNm as shown on Figure 3.3 and represented by equivalent force couple as shown in figure 3.4.

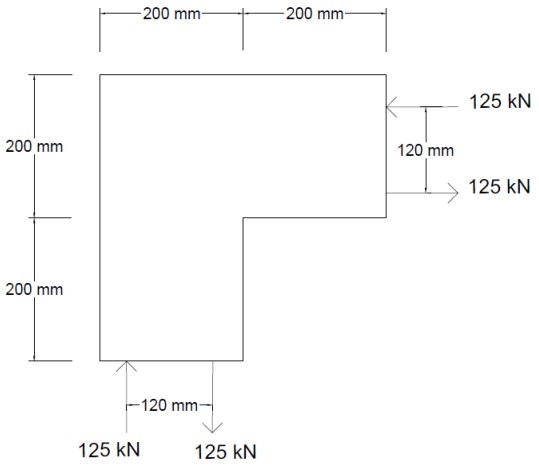

Figure 3. 4 Resultant forces acting on D-region (scheme-1)

With the resultant forces acting on the boundary now determined, the next step is essentially placing a truss within the D-region to carry the forces through it. The model used is compatible with the actual stress flow in the structure. The truss model consists of struts to carry compressive stresses, ties to carry tensile stresses and nodes where three or more struts and/or ties meet. The proposed strut and tie model for this section is shown in Figure 3.5.

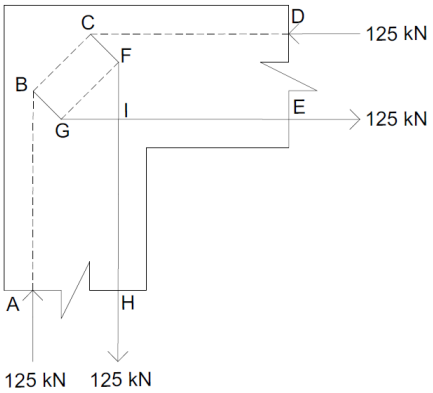

Figure 3. 5 Proposed strut and tie model for scheme-1

In figure 3.5, the strut (dotted line) models the compressive stress flow while the tie (solid line) models the tensile stress flow in the section in response to the applied loads. Nodes occur where three or more struts and/or ties meet. Ties are allowed to cross each other without a node, hence there is no node at 'I'. The nodes in Figure 5.4 are B, G, C and F. The node is essentially a volume of concrete in the region where struts and/or ties meet, and thus has defined geometric dimensions. The dimensions of the nodes, struts and ties was determined based on the forces they are subjected to and their material strength. Treating the nodes as pinned joint, and applying the conditions for equilibrium i.e. $\sum F_x = 0$, $\sum F_y = 0$ and $\sum M = 0$, the internal force distribution was obtained using the method of joint resolution from structural analysis. The computed internal forces in the struts and tie of the D-region are presented in Figure 3.6.

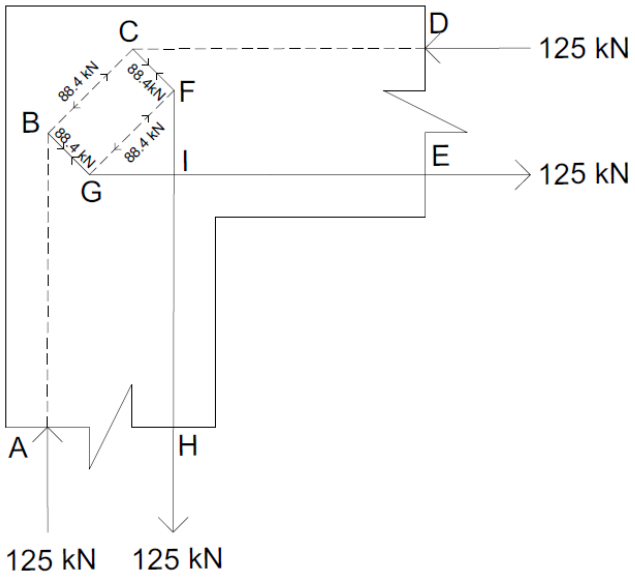

Figure 3. 6 Internal forces in strut and tie model (scheme-1)

Note that the angle between the ties and the inclined strut at nodes B and E is 45 degrees, thus well within the requirements of EC2.

Dimensioning of nodes, struts and ties

The concept of non- hydrostatic node is used to dimension the nodes, struts and ties in this section. Non hydrostatic node implies ensuring that the maximum stress on the face of a node to the minimum stress should be less than 2.

Node B

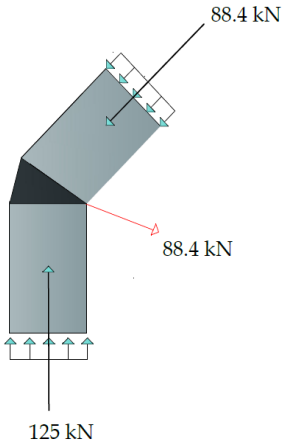

Figure 3. 7 Forces acting on Node B

The three forces acting on node B are illustrated in Figure 3.7. It is a CCT node, this node is compressed on the two faces and tensioned on the other face of the node. The maximum strength of the node from EC2 is determined using equation (2.7):

$$\sigma_{Rd,\max} = k_i \cdot \left[1 - \frac{f_{ck}}{250}\right] \cdot f_{cd}$$

Where k_i is 0.85 for a CCT node. Thus, the nodal strength is:

$$\sigma_{Rd,\max} = 0.85 \cdot \left[1 - \frac{30}{250}\right] \cdot 20 = 14.96 MPa$$

Struts BA and BC

Strut BA is in uniaxial compression, thus its strut strength is determined using equation (2.4) as follows:

$$\sigma_{Rd,\max} = \alpha_{cc} \frac{f_{ck}}{\gamma_c} = 0.85 \cdot \frac{30}{1.5} = 17.0 MPa$$

A value of 0.85 is used for α_{cc} in calculating the concrete compressive strength above. This value is used to account for long term effects.

Strut BC is bottle-shaped and the strength is determined using equation (2.5) as follows:

$$\sigma_{Rd,\max} = 0.6 \cdot \left[1 - \frac{f_{ck}}{250}\right] \cdot f_{cd}$$

$$\sigma_{Rd,\max} = 0.6 \cdot \left[1 - \frac{30}{250}\right] \cdot 20 = 10.56 MPa$$

Using the above calculated strengths, the nodes should be dimensioned such that the maximum stress on any nodal face should not exceed the calculated strengths.

The capacity of the nodal face can be obtained using equation (2.3):

$$F_{cu} = A_c \cdot \sigma_{Rd,\max}$$

$$A_c = w \cdot t$$

Where F_{cu} is the compressive force acting on that nodal face, and A_c is the area of the nodal face. w and t, represent width and thickness respectively. The minimum width of the nodal face is thus obtained using:

$$w_i = \frac{F_{cu}}{\sigma_{Rd,\max} \cdot t} \text{ , t=160mm}$$

$$w_{BA} = \frac{125 \cdot 10^3}{14.96 \cdot 160} = 52.2 mm$$

$$w_{BC} = \frac{88.4 \cdot 10^3}{14.96 \cdot 160} = 36.97 mm$$

$$w_{BG} = \frac{88.4 \cdot 10^3}{14.96 \cdot 160} = 36.97 mm$$

The minimum base dimension of node B and the width of strut BA is 36.97mm and 52.2mm respectively. The numbers are less than half the width of the joint. So the node could easily fit within the dimensions of the joint. Thus the node is not stressed beyond the design limit.

The capacity of the struts can be dimensioned using equation (2.3) as follows:

$$w_i = \frac{F_{cu}}{\sigma_{Rd,\max} \cdot t} \text{ , t=160mm}$$

$$w_{BA} = \frac{125 \cdot 10^3}{17 \cdot 160} = 45.95 mm$$

$$w_{BC} = \frac{88.4 \cdot 10^3}{10.56 \cdot 160} = 52.32mm$$

Node F

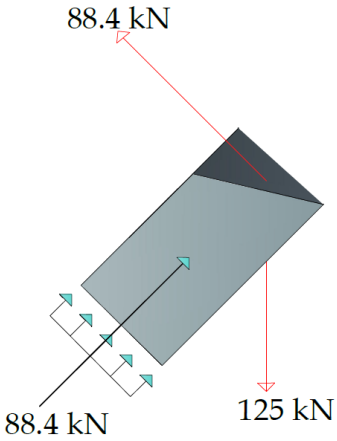

Figure 3. 8 forces acting on Node F

The node is a CTT node. For the Node, the maximum allowable stress is obtained from equation (2.5):

$$\sigma_{Rd,\max} = k_i \cdot \left[1 - \frac{f_{ck}}{250}\right] \cdot f_{cd}$$

Where k_i= 0.75 for CTT node. Therefore, nodal strength is:

$$\sigma_{Rd,\max} = 0.75 \cdot \left[1 - \frac{30}{250}\right] \cdot 20 = 13.2MPa$$

For the strut, the strength is determined using equation (2.4):

$$\sigma_{Rd,\max} = \alpha_{cc} \cdot \frac{f_{ck}}{\gamma_c} = 0.85 \cdot \frac{30}{1.5} = 17MPa$$

The expression that was used for node B is also applicable for this case. Thus the minimum width of components in node F would be obtained using equation (2.3):

$$w_i = \frac{F_{cu}}{\sigma_{Rd,\max} \cdot t}\ , \text{t=160mm}$$

$$w_{FH} = \frac{125 \cdot 10^3}{13.2 \cdot 160} = 59.18mm$$

$$w_{FG} = \frac{88.4 \cdot 10^3}{13.2 \cdot 160} = 41.85mm$$

$$w_{FC} = \frac{88.4 \cdot 10^3}{13.2 \cdot 160} = 41.85mm$$

Thus the node is non- hydrostatic and the node could easily fit within the dimensions of the joint.

The dimensions of the struts and nodes are summarized in Table 2.1 and Table 2.2 below.

Table 2. 1 Dimensioning of struts for scheme-1

Member designation	type	Axial force (kN)	Limiting compressive strength, MPa	Minimum width, mm	width provided, mm	Remark
AB	strut	125	17.00	45.96	60.00	O.K
BC	strut	88.4	10.56	52.32	84.90	O.K
CD	strut	125	17.00	45.96	60.00	O.K
GF	strut	88.4	10.56	52.32	84.90	O.K

Table 2. 2 Dimensioning of nodes for scheme-1

Node designation	K	Type of node	element	Axial force (kN)	Minimum width, mm	Width provided, mm	Remark
B	0.85	CCT	BA	125	52.22	60	O.K
			BC	88.4	36.93	84.9	O.K
			BG	88.4	36.93	84.9	O.K
C	0.85	CCT	CB	125	52.22	60	O.K
			CD	88.4	36.93	84.9	O.K
			CI	88.4	36.93	84.9	O.K
F	0.75	CTT	FG	88.4	41.86	84.9	O.K
			FD	88.4	41.86	84.9	O.K
			FI	125	59.19	60	O.K

G	0.75	CTT	GF	88.4	41.86	84.9	O.K
			GH	88.4	41.86	84.9	O.K
			GA	125	59.19	60	O.K

Bottle-shaped strut BC

Strut BC, a bottle-shaped strut connecting node B and C, is critical to the performance of the joint. Apart from the axial compressive forces in the strut, there is also some transverse tensile stresses which could actually cause cracking longitudinally along the axis of the strut. These transverse cracks actually reduce the compressive strength of the strut. This was taken into account in the calculation of the concrete strength. However, the presence of transverse tensile stresses in the strut is still a concern, as it is the primary cause of diagonal tension cracking failure discussed in section 2.2.2. The diagonal tension force would be estimated next using expressions from section 6.5.3 of EC2. Figure 3.9 illustrates the parameters used to compute the transverse tension force to be resisted.

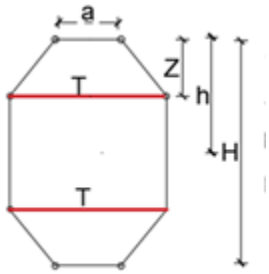

Figure 3. 9 Dimensions of the bottle-shaped strut BC

a=52.3 mm, (width of bottle shaped strut BC)

H=84.9mm (length of strut taken from drawing)

h=42.425mm (h=H/2)

Z=21.2mm, (z=h/2)

The joint region in this case is fully disturbed, for such a fully discontinuous region equation (2.2) is used to compute the transverse tension:

$$T = \frac{1}{4} \cdot \left(1 - 0.7\frac{a}{h}\right) \cdot F$$

$$T = \frac{1}{4} \cdot \left(1 - 0.7\frac{52.3}{42.42}\right) \cdot 88.4 = 3.02kN$$

Thus a tension force of 3.02kN is estimated from the transverse tensile stresses within a joint.

In order to prevent diagonal tension cracking failure from these tensile stresses, methods such as, bending the main reinforcement into a loop, use of inclined stirrups to control the cracks and use of bent bar to cross the strut path could be used.

Reinforcement design

The required area of steel for the tie is calculated using equation (2.6) as follows,

Axial Tensile force, $F_{HF}=F_{GE}=125kN$

$$\text{Therefore, } A_s = \frac{F_{HF}}{f_{yd}} = \frac{125 \cdot 10^3}{347.8} = 359.4mm^2$$

Axial Tensile force, $F_{BG}=F_{CF}=88.4kN$

$$\text{Therefore } A_s = \frac{F_{CF}}{f_{yd}} = \frac{88.4 \cdot 10^3}{347.8} = 254.15mm^2$$

As for the transverse ties, $F_{HF=}3.02kN$

$$\text{Therefore, } A_s = \frac{F_{BC}}{f_{yd}} = \frac{3.02 \cdot 10^3}{347.8} = 8.7mm^2$$

While the reinforcements for ties FH, GE, BG and CF are primary reinforcements, the ties due to transverse tension in the bottled shaped strut BC are secondary reinforcements and may not be used in some structural details. Where looped reinforcement is used in the joint, there may be no need for this reinforcement.

Accordingly, for the loop reinforcement (RL1), since the primary reinforcement bar will be bent $180^{0,}$ 2ϕ16mm diameter bars will be provided for the tensile reinforcement. In addition, 2ϕ10mm diameter bars will be provided as stirrup hangers (Refer Figure 3.10).

For the hair pin reinforcement with stirrups, 2ϕ16mm diameter bars will be provided for the straight bars and 2ϕ14 stirrups in the diagonal. In addition, 2ϕ10mm diameter bars will be provided as stirrup hangers (Refer Figure 3.11).

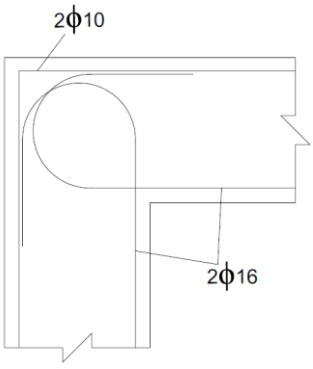

Figure 3. 10 Reinforcing bars for RL1

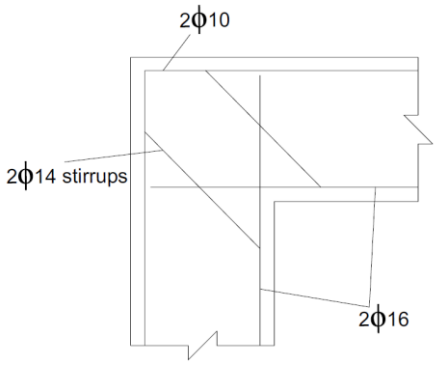

Figure 3. 11 Reinforcing bars for RL2

3.2.2 Strut and tie analysis of the joint, scheme -2

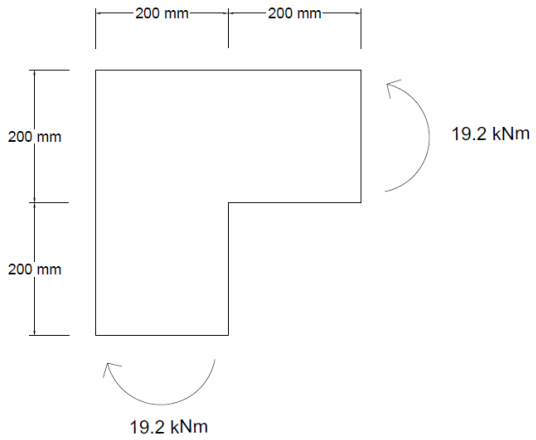

Figure 3. 12 Delineated D-region of a beam-column joint (scheme-2)

In this section, the delineated D-region of Figure 3.12 is analyzed using the strut-and-tie method. The sequence of steps followed in section 3.2.1 in strut and tie design is also followed in this section.

The resultant forces caused by the moment, are calculated as a pair of forces. The resultant forces acting on the D-region are depicted in Figure 3.13

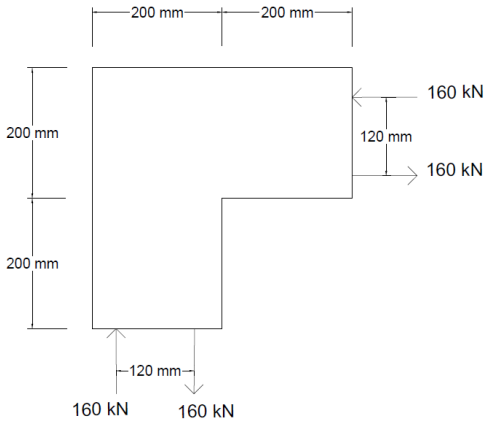

Figure 3. 13 Resultant forces acting on D-region (scheme-2)

With the resultant forces acting on the boundary now determined, the next step is essentially placing a truss within the D-region to carry the forces through it. The proposed strut and tie model for this section, as recommended by Eurocode is shown in figure 3.14.

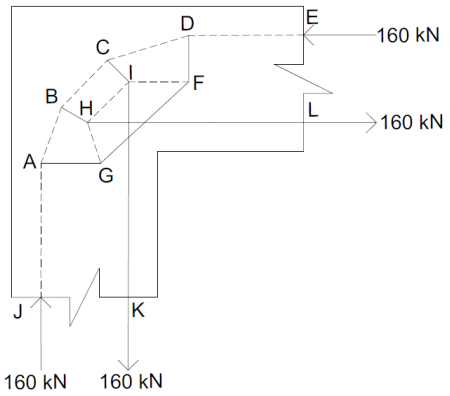

Figure 3. 14 Proposed strut and tie model for scheme-2

The internal force distribution obtained using the method of joint resolution is presented in figure 3.15.

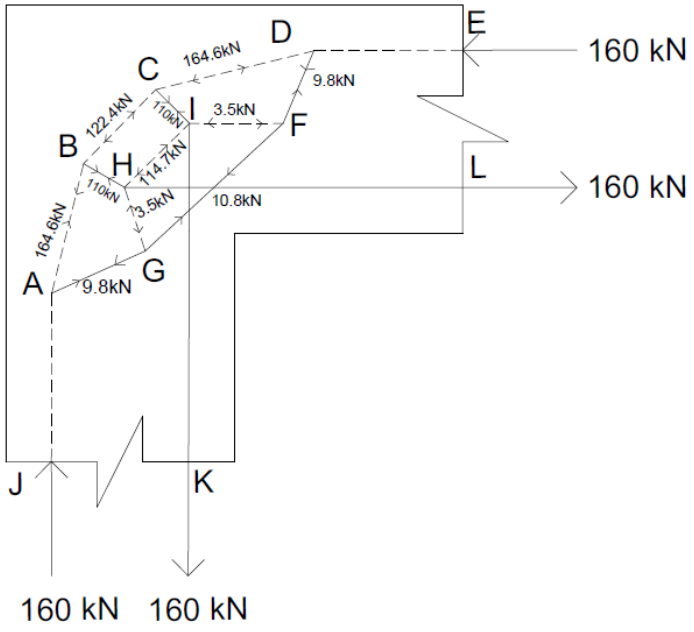

Figure 3. 15 Internal forces in strut and tie model (scheme-2)

Dimensioning of nodes, struts and ties

The nodes, struts and ties are dimensioned in this section. However, since the calculation was illustrated in the previous section, only tabulated results will be presented below in Table 2.3 and Table 2.4

Table 2. 3 Dimensioning of struts for scheme-2

Member designation	Type	Axial force (kN)	Limiting compressive strength, $\sigma_{Rd,max}$ MPa	Minimum width, mm	width provided, mm	Remark
AJ	strut	160	17.00	58.82	120.00	O.K
AB	strut	164.6	17.00	40.34	56.80	O.K
BC	strut	122.4	10.56	72.44	76.40	O.K
CD	strut	164.6	17.00	40.34	56.80	O.K
DE	strut	160	17.00	58.82	120.00	O.K
GH	strut	3.5	10.56	2.07	15.30	O.K
HI	strut	114.7	10.56	67.89	76.40	O.K
IF	strut	3.5	10.56	2.07	15.30	O.K

Table 2. 4 Dimensioning of nodes for scheme-2

Node designation	K	Type of node	Element	Axial load, kN	Minimum width required, mm	Width provided, mm	Remark
A	0.85	CCT	AJ	160	66.84	120	O.K
			AB	164.6	68.77	102.5	O.K
			AG	9.8	4.09	196.1	O.K
B	0.85	CCT	BA	164.6	55.01	56.8	O.K
			BC	122.4	51.14	76.4	O.K
			BH	110	45.96	76.4	O.K
C	0.85	CCT	CB	122.4	51.14	76.4	O.K
			CD	164.6	55.01	56.8	O.K
			CI	110	45.96	76.4	O.K
D	0.85	CCT	DC	164.6	68.77	102.5	O.K
			DE	160	66.84	120	O.K
			DF	9.8	4.09	196.1	O.K
F	0.75	CTT	FG	10.8	5.11	20.5	O.K
			FD	9.8	4.64	32.4	O.K
			FI	3.5	1.66	15.3	O.K
G	0.75	CTT	GF	10.8	5.11	20.5	O.K

			GH	3.5	1.66	15.3	O.K
			GA	9.8	4.64	32.4	O.K
H	0.75	CTT	HL	160	50.51	54	O.K
			HB	110	52.08	76.4	O.K
			HG	3.5	1.66	76.4	O.K
			HI	114.7	54.31	56.9	O.K
I	0.75	CTT	IK	160	50.51	54	O.K
			IH	114.7	54.31	76.4	O.K
			IC	110	52.08	76.4	O.K
			IF	3.5	1.66	56.9	O.K

Reinforcement design

The required area of steel for the tie is calculated using the formula given in equation 2.6,

Axial Tensile force, F_{AG}= F_{FD}=9.8kN

$$\text{Therefore, } A_s = \frac{F_{AG}}{f_{yd}} = \frac{9.8 \cdot 10^3}{347.8} = 28mm^2$$

Axial Tensile force, F_{GF}=10.8

$$\text{Therefore, } A_s = \frac{F_{GF}}{f_{yd}} = \frac{10.8 \cdot 10^3}{347.8} = 31mm^2$$

Axial Tensile force, F_{BH}=F_{CI}=110.0kN

$$\text{Therefore, } A_s = \frac{F_{BH}}{f_{yd}} = \frac{110 \cdot 10^3}{347.8} = 316.27mm^2$$

Axial Tensile force, F_{KI}=F_{HL}=160kN

$$\text{Therefore, } A_s = \frac{F_{KI}}{f_{yd}} = \frac{160 \cdot 10^3}{347.8} = 460.03mm^2$$

For the hair pin reinforcement with stirrups and diagonal bars (RL3), 2ϕ20 mm diameter bars will be provided for the straight bar. For the diagonal bar 1ϕ8 mm bar should be provided. However, Karlsson (1999) recommends to provide diagonal bars with an amount of about one-half of the main reinforcement, A_s. In addition, according to Nillson (1975) and Jhonnson(2000) an area that is equal to half the area of the main tensional bar should be provided as diagonal bars. Accordingly 1 ϕ20mm diagonal bar was provided and 3 ϕ12 stirrups in the diagonal. In addition, 2ϕ10mm diameter bars are provided as stirrup hangers.

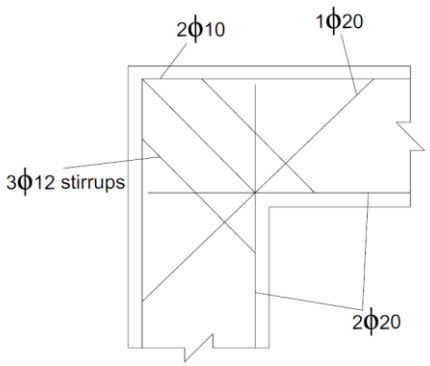

Figure 3. 16 Reinforcing bars for RL3

For the loop reinforcement with diagonal bars (RL4), (Figure 3.17) since the primary reinforcement bar will be bent $180^{0,}$ 2ϕ20mm diameter bars will be provided for the whole tensile reinforcement and 1 ϕ20 for diagonal bar. In addition, 2ϕ10mm diameter bars are provided as stirrup hangers.

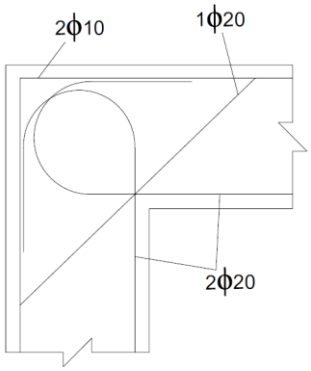

Figure 3. 17 Reinforcing bars for RL4

3.3 Moment capacity of the member

The desired scenario in design occurs where the joint is stronger than the connected members i.e. the joint does not prevent the connected member from reaching their design capacity. In the next chapter, the flexural strength of the frame will be used as a reference strength to assess the efficiency of joint reinforcement details. Moment capacity for the member is calculated according to mechanics as follows.

$$M_{cal} = \rho \cdot b \cdot d^2 \cdot f_y \cdot \left[1 - \frac{\rho \cdot f_y}{2 \cdot f_{cp}}\right]$$

where ρ refers to the geometrical reinforcement ratio (cross-sectional area of the reinforcement divided by the width and effective depth of the section), f_y refers to the yield strength of the reinforcement and f_{cp} to the plastic strength of concrete ($f_{cp} = fc \cdot \eta_{fc}$, where fc is the compressive strength of concrete measured in cylinder and η_{fc} a brittleness factor: $\eta_{fc} = (30/fc\ [MPa])^{1/3} \leq 1$). (Muttoni A, Schwartz J, Thürlimann B.(1996), Fernández Ruiz M, Muttoni (2007))

N.B. Even though the joints were designed for specific moments, the areas provided were higher than calculated. Due to this discrepancy, there was a need to calculate the actual moment capacity of the connected member reinforced with the reinforcement area provided.

b = 160mm; d = 160mm; f_{yd}= 347.8 MPa f_c= 30 MPa

For scheme-1

$$\rho = \frac{A_s}{b \cdot d} = \frac{402.12}{160 \cdot 160} = 0.0157$$

$$f_{cp} = f_c \cdot \eta_{fc}; \eta_{fc} = \sqrt[3]{\frac{30}{30}} \leq 1$$

$$f_{cp} = 30 \cdot 1 = 30MPa$$

$$M_{cal} = 0.0157 \cdot 160 \cdot 160^2 \cdot 347.8\left[1 - \frac{0.0157 \cdot 347.8}{2 \cdot 30}\right] = 20.33kNm$$

The above calculated moment capacity of 20.33kNm will serve as a reference to which the joint capacity would be compared to in 'Reinforcement layout 1, RL1' and 'Reinforcement lay out 2, RL2' in the next chapter.

For scheme-2

$$\rho = \frac{A_s}{b \cdot d} = \frac{628.31}{160 \cdot 160} = 0.025$$

$$f_{cp} = f_c \cdot \eta_{fc}; \eta_{fc} = \sqrt[3]{\frac{30}{30}} \leq 1$$

$$f_{cp} = 30 \cdot 1 = 30MPa$$

$$M_{cal} = 0.025 \cdot 160 \cdot 160^2 \cdot 347.8\left[1 - \frac{0.025 \cdot 347.8}{2 \cdot 30}\right] = 29.95kNm$$

The above calculated moment capacity of 29.95kNm will serve as a reference to which the joint capacity would be compared to in 'Reinforcement layout 3, RL3' and 'Reinforcement lay out 4, RL4' in the next chapter.

4. Nonlinear Finite Element Analysis of a Corner Joint

FEM is a numerical technique to find approximate solutions for boundary value problems, for partial differential equations and also for integral equations. Finite Element Analysis (FEA) represents a numerical method, which provides solution to problems that would otherwise be difficult to obtain. The numerical analysis investigations were performed using VecTor2, a nonlinear finite element analysis program that utilizes two-dimensional continuum elements. This software is a suite of powerful engineering simulation programs, based on finite element method, which can solve problems ranging from relatively simpler linear analyses to the most challenging non-linear simulations. The analysis of a structure with VecTor2 is performed in three stages; Pre-processing, Analysis solver and Post-processing.

In this chapter, the nonlinear finite element analysis of corner joints designed using the strut and tie model in Chapter 3 is presented.

4.1 VecTor2 Analytical Procedure

The nonlinear finite element software explored in this study is VecTor2, a two dimensional nonlinear finite element analysis program for reinforced concrete structures developed at the University of Toronto. VecTor2 is based on the Modified Compression Field Theory (MCFT) by Vecchio and Collins (1986) and the Distributed Stress Field Model (DSFM) by Vecchio (2000). VecTor2 is capable of modeling two-dimensional reinforced concrete membrane structures under monotonic, cyclic and reversed cyclic loading conditions. The element library of the program is limited. However, the element library covers many of the required elements for reinforced concrete structures. More importantly, it uses state-of-the-art material models for concrete, reinforcing and prestressing steel.

The MCFT is based on a smeared, rotating crack model for reinforced concrete, in which cracked concrete is represented as an orthotropic material with a unique constitutive relation. VecTor2 is a nonlinear finite element program that utilizes an incremental total load and iterative secant stiffness algorithm to produce an efficient and robust nonlinear solution. Additional information on VecTor2 program is given in 'VecTor2 & FormWorks User's Manual'' by Wong (2002). Furthermore, the details of the constitutive models and their implementation into VecTor2 software have been described by Vecchio (2000).

4.1.1 Concrete

VecTor2 uses three node constant strain triangular elements with six degrees of freedom and four-node plane stress rectangular elements with eight degrees of freedom to model concrete with distributed reinforcement. Plain as well as reinforced concrete with smeared reinforcement can be modeled using these elements. In VecTor2 program, various constitutive and behavioral models are available for concrete. The concrete model in VecTor2 accounts for the reduction of compressive strength and stiffness due to transverse cracking and tensile straining. Concrete tension stiffening, crack shear slip, concrete tension splitting, concrete confinement and concrete dilatation can be considered in the analysis. Description of these effects is out of the scope of this paper and details of all these options are available in VecTor2 user's manual (Wong and Vecchio 2003). The behavioral models that were used for the concrete are given in Table 4.1. The default models were chosen for the parameters used in modeling both concrete and reinforcement.

Table 4. 1: Material Behavior Models for Concrete

Material Property	Model
Concrete Compression Pre-Peak Response	Hognestad Parabola
Concrete Compression Post-Peak Response	Modified Park-Kent
Concrete Compression Softening	Vecchio 1992-A (e1/e2-Form)
Concrete Tension Stiffening	Modified Bentz 2003
Concrete Tension Softening	Bilnear
Concrete Confined Strength	Kupfer/Richard Model
Concrete Dilation	Variable isotropic
Concrete Cracking Criterion	Mohr-Coulomb (Stress)
Concrete Crack Slip Check	Vecchio-Collins 1986
Concrete Crack Width Check	Agg/2.5 Max Crack Width

4.1.2 Steel Rebar

Reinforcement can be modeled using either a smeared or a discrete representation. When the longitudinal or transverse bars are sufficiently well distributed, smeared reinforcement is appropriate. Smeared reinforcement can be defined based on rebar percentage and rebar direction. The smeared reinforcement layer behaves as a unidirectional (in the specified direction) material. In order to model the discrete reinforcement, two-node truss bar element with four degrees of freedom is used.

The constitutive relationship used for reinforcing steel is based on a trilinear stress–strain behavior. The strain hardening effect of reinforcement until rupture is considered in VecTor2. Dowel action as well as reinforcement buckling can be considered in the analytical model using VecTor2. In this study, transverse rebar (stirrups) are modeled based on the smeared option, and all longitudinal reinforcement are modeled using truss elements. Although bond slip between concrete and rebar is modeled using link element, perfect bond has been assumed for this element. This means that no slip is considered between the bar truss elements and the concrete elements.

Table 4. 2 Material Behavior Models for Reinforcement

Material Property	Model
Reinforcement Dowel Action	Tassios Model (Crack Slip)
Reinforcement Buckling	Akkaya 2012 (Modified Dhakal-Maeka)

4.1.3 Geometry and Meshing

Due to the rectangular shape of the beam–column subassembly, only the rectangular concrete element is used for the finite element modeling of the subassembly. Because transverse reinforcements in the beam and column are not the same, different concrete materials are assigned to these parts. Rectangular stirrups are replaced by smeared reinforcement in two perpendicular directions. Mild steel properties are used to model the steel plate. Figure 4.1 shows the divided regions of beam–column sub- assembly based on their material properties.

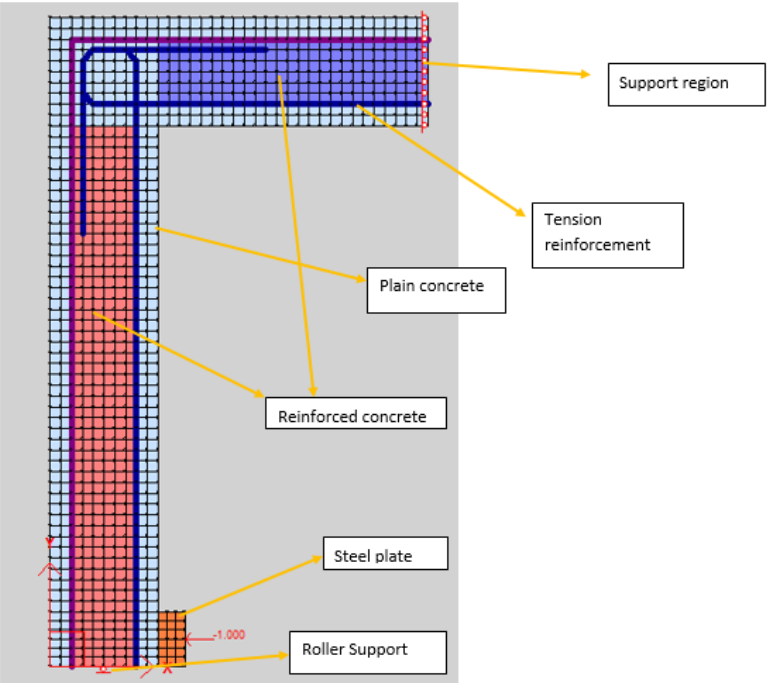

Figure 4. 1 Element mesh and different material regions in VecTor2

4.2 verification

In order to validate the accuracy and reliability of the numerical model, numerical analysis of a reinforced concrete corner joints under opening moments were performed using VecTor2 and the numerical results are compared with those reported by the authors.

The experimental results of a case study by 'Nilsson (1973)', 'Nabil et al. (2014)' and 'Roshan et al. (2015) are considered, and the VecTor2 FEM is employed to create two-dimensional models for corner joints within the context of the finite element method. The nonlinear response is traced throughout the entire load range up to failure.

1. **Experimental test setup**

The loading arrangement of the test specimens for the case studies are shown from Figure 4.2-Figure 4.4.

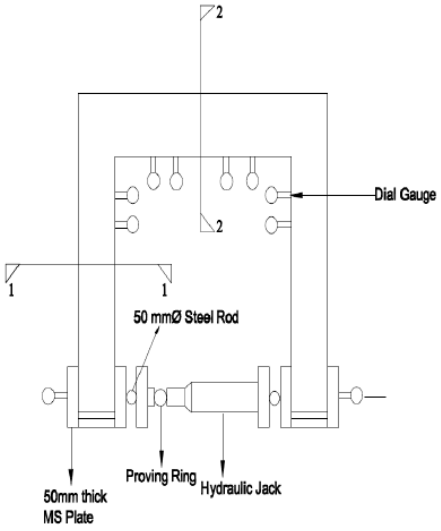

Figure 4. 2 Loading arrangement of the test specimens by Roshan et al. (2015)

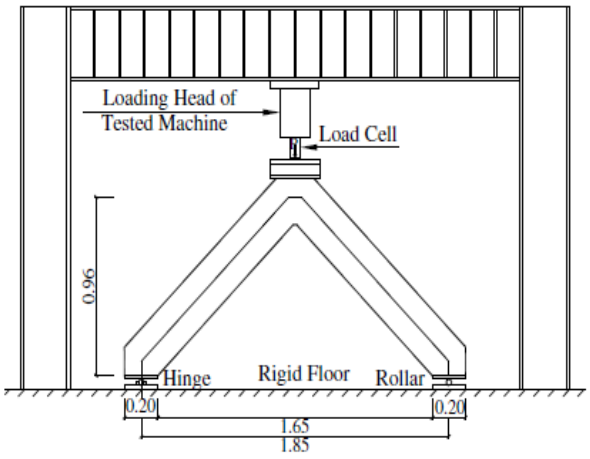

Figure 4. 3 Dimensions and method of loading of test model for Nabil et al. (2014)

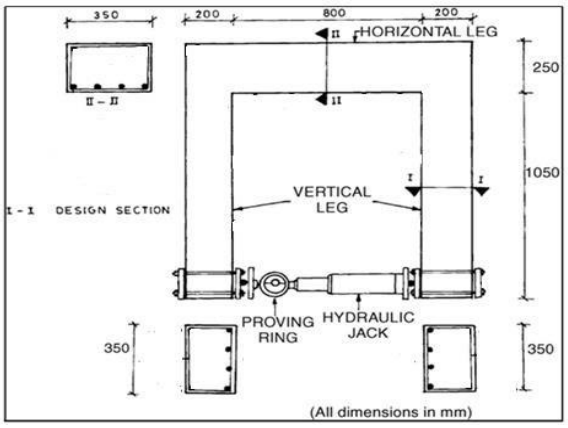

Figure 4. 4 Loading arrangement of the Nilsson's (1973) test specimens

2. Reinforcement details investigated in the case studies

The reinforcement details investigated for each case study is shown below from Figure 4.5-Figure 4.7.

Figure 4. 5 Reinforcement details by Roshan et al. (2015)

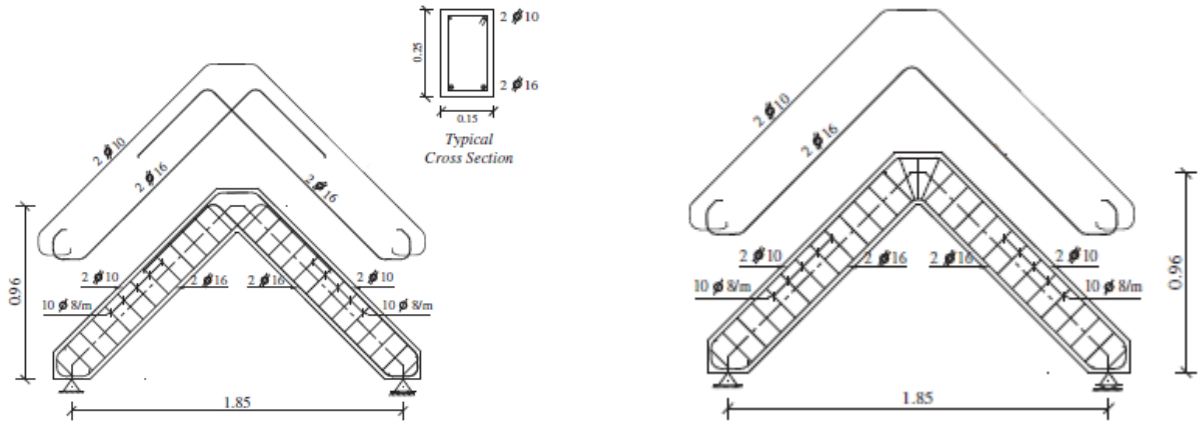

a) F1 b) F4

Figure 4. 6 Reinforcement details by Nabil et al. (2014)

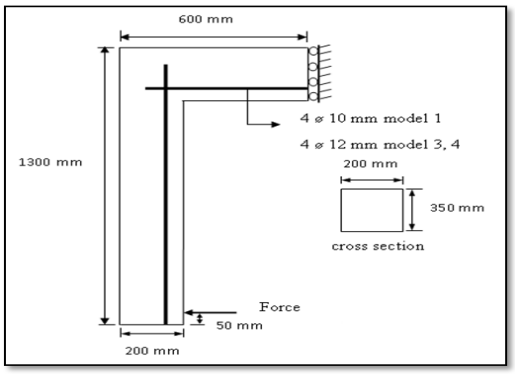

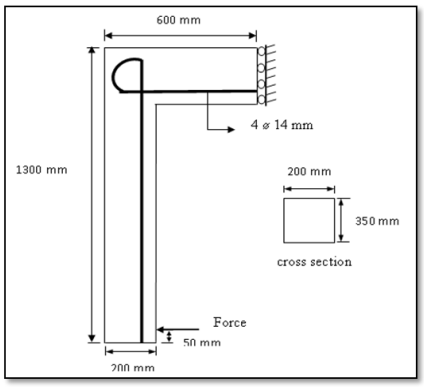

a) H1A b) L1

Figure 4. 7 Nilsson's (1973) reinforcement details

3. Models

Shown from Figure 4.8- Figure 4.11 below are the models used for the VecTor2 analysis.

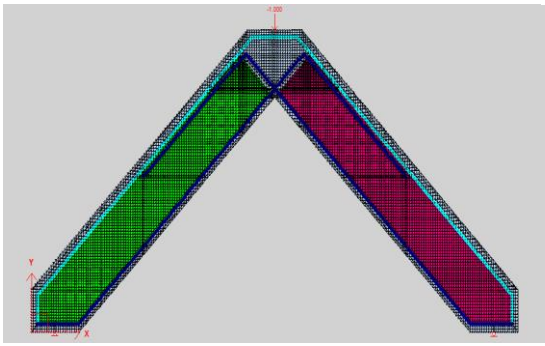

Figure 4. 8 Model for F1

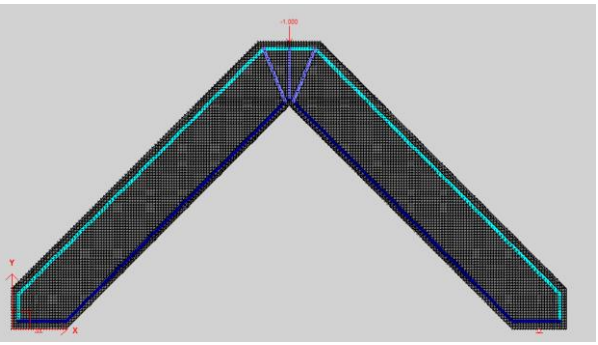

Figure 4. 9 Model for F4

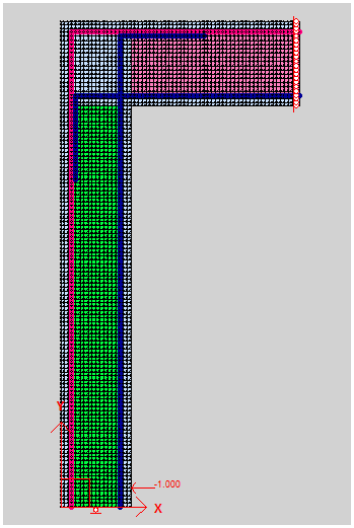

Figure 4. 10 Model for SP1

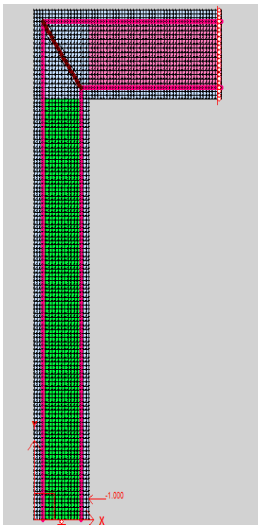

Figure 4. 11 Model for SP2

4. Results

The results obtained from the VecTor2 analysis are tabulated in the tables below:

Table 4. 3 FEM results of reinforcement details by Roshan et al. (2015)

Designation of corners	f_{cu}, MPa	% tension reinforcement	Test failure moment , M_{ut} in kNm	VecTor2 failure moment , M_{uv}, in kNm	M_{uv}/M_{ut}
SP1	37.52	0.76	5.4	5.64	1.04
SP2	39.24	0.76	7.14	7.22	1.01

Table 4. 4 FEM results of reinforcement details by Nabil et al. (2014)

Frame	Test failure loads (kN)	M_{ut}, test failure moment (kNm)	VecTor2 failure load, kN	VecTor2 failure moment , M_{uv}, in kNm	M_{ut}/M_{uv}
F1	62.12	28.72	61.4	28.43	1.01
F4	35.97	16.63	32.96	14.80	1.09

Table 4. 5 FEM results of reinforcement details by Nillson's (1973)

Designation of corners	f_{cu}, MPa	% tension reinforcement	Test failure moment , M_{ut} in kNm	VecTor2 failure moment , M_{uv}, in kNm	M_{uv}/M_{ut}
H1B	28	0.75	22.27	23.9	1.07
S1A	32	0.75	24.74	26.2	1.06

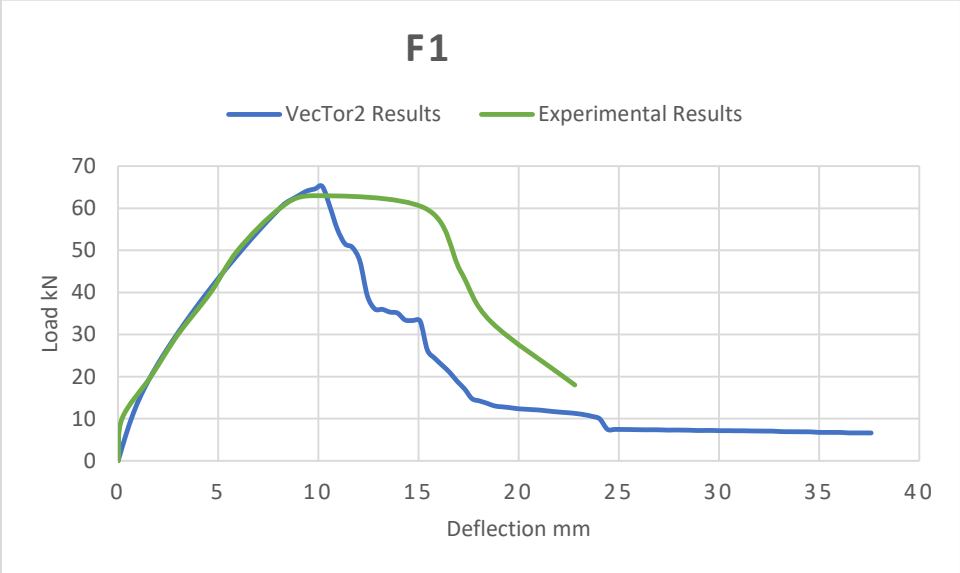

Figure 4. 12 comparison of results of FE and tests for F1 of Nabil et al. (2014)

It can be seen that the FE model captured the structural behavior in a satisfactory way. The maximum moment resistances obtained in the FE analyses are equal to those obtained in the tests

to within 10% difference, as shown in Tables 4.3-4.5. Figure 4.12 shows a comparison between load and lateral deflection curves of the finite element analysis and experimental result obtained for specimens F1 in Nabil et al. (2014) experiment .The model agreed well with the test results in terms of failure loads as well as the deformation.

Therefore, it can be realized that VecTor2 software realistically simulates corner joints subjected to opening moments.

4. 3 Finite Element Analysis of the corner joint

In the previous chapter, a preliminary analysis for the D-region of the corner joint was studied using strut-and-tie methodology. The position and general layout of reinforcing steel play a vital role in the behavior of the joint. Due to concrete's low strength in tension, steel is often relied on as the main tensile member in reinforced concrete (with the concrete strength usually ignored in design). Thus the steel layout plays a role in determining tensile stress and strain distribution within the joint, its failure mode, and even its ultimate capacity.

In this chapter, VecTor2 finite element software is used to study different aspects and variants of reinforcement detailing for the D-region. The Specific question of interest is "How does a reinforcement detail affect the behavior and capacity of a corner joint?"

Material parameters used:

For concrete the material parameters used are:

$f_{ck} = 30MPa$; $f_{ctd} = 1.35MPa$; $E_c = 33{,}000MPa$; $\nu = 0.2$

For tensile behavior: bilinear softening model with fracture energy, $G_f = 75N/m$.

For steel: The material design strength, $f_{yd} = 347.8MPa$ and the modulus, $E_s = 200{,}000MPa$.

For the composite action of concrete and steel, perfect bond is assumed to exist.

The tensile reinforcement ratio in legs is $\rho = 1.57$ % for RL1 and RL2, and $\rho = 2.45\%$ for RL3 and RL4.

Table 4. 6 Models designation and their properties

Group	**Specimen designation**	**Longitudinal reinforcement**	**Transverse reinforcement**
1	RL1	$2\phi 16$ tensile,	
		$2\phi 10$ stirrup hangers	$\phi 8c/c100mm$

	RL2	2 ϕ 16 tensile 2 ϕ 14 inclined stirrups	$\phi 8c/c100mm$
		2 ϕ 10 stirrup hangers	
2	RL3	2 ϕ 20 tensile 1 ϕ 20 diagonal bar	$\phi 8c/c100mm$
		2ϕ 10 stirrup hangers	
	RL4	2 ϕ 20 tensile 3 ϕ 12 inclined stirrups 1 ϕ 20 diagonal bar	$\phi 8c/c100mm$
		2 ϕ 10 stirrup hangers	

Model description:

The models are designed to represent an actual prototype of a portal frame corner shown in Figure 4.13 a. Since the structure is symmetrical, only half of the section is modelled (Figure 4.13 b). The nominal dimensions of the modelled corners are 1200 mm in vertical height, 700 mm in horizontal length and 150mm in thickness, and the effective depth for all corner's leg section is held constant at 160 mm.

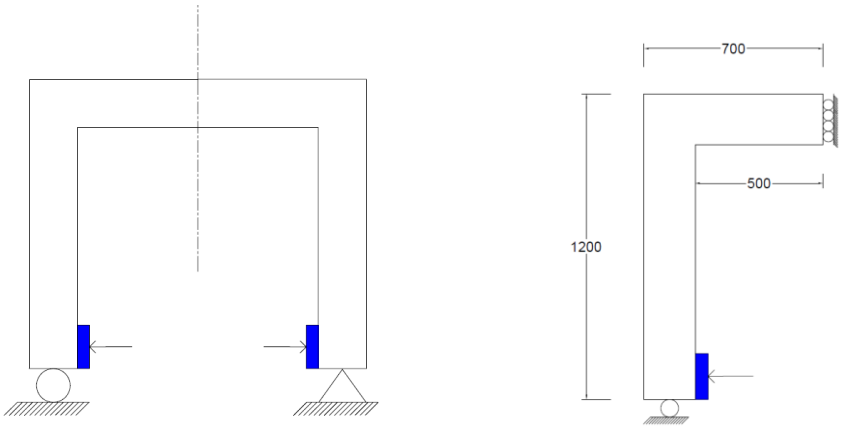

a) portal frame b) sectioned portal frame

Figure 4. 13 geometrical model used for FEM (dimensions are in mm)

Loading:

The structure is idealized as being weightless with the loads on the structure applied as imposed displacement. The imposed displacement was applied to a node placed at 60mm above the bottom of the column. The imposed displacement was not applied directly to the column to prevent local crushing at the point of action. Rather, a steel plate was used. With this loading layout, no local crushing occurred at the point of load application.

4.3.1 Preliminary study

A key objective in the joint design is for the beam and the column to interact effectively together so that the structure achieves its full capacity. That interaction between the beam and column depends (to a great extent) on the reinforcement layout. To begin this study, a conventional detailing layout where the tensile reinforcements are bent 90^0, will be studied first (refer Figure 4.14). Though this is not one of the recommended layouts in the Eurocode, it is used in practice. Hence, it is a good starting point for this study.

This solution was common before the extensive experimental studies carried out in the late sixties and early seventies (e.g. Swann 1969; Mayfield et al. 1971, 1972; Balint and Taylor 1972; and Nilsson 1973) that showed its substantial shortcoming. It was found that this detailing was far from satisfactory, resulting in efficiencies (i.e. the ratio of the measured capacity divided by the calculated capacity in the adjoining members) as low as 8%. For this preliminary study, a section reinforced by 2ϕ 16 bars for tension is modelled and the behavior is analyzed.

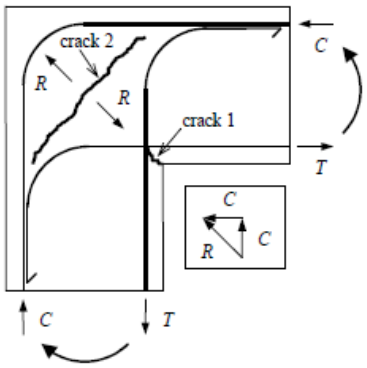

Figure 4. 14 Reinforcement layout in earlier practice

The stress distribution in this joint region is quite complex when compared to that of the adjacent B-region in the frame. Hence, Understanding the stress state is vital to this study, as it depicts how the structure tries to distribute the load among its members, and how interaction between the beam and column is achieved.

The observed behavior of the frame is described as follows: Prior to the occurrence of the first crack, the load-displacement behavior was linear as shown in Figure 4.15. The structure behaved like an elastic isotropic material. But after the first crack, the stress distribution in the joint became quiet complex as compared to that of the B region.

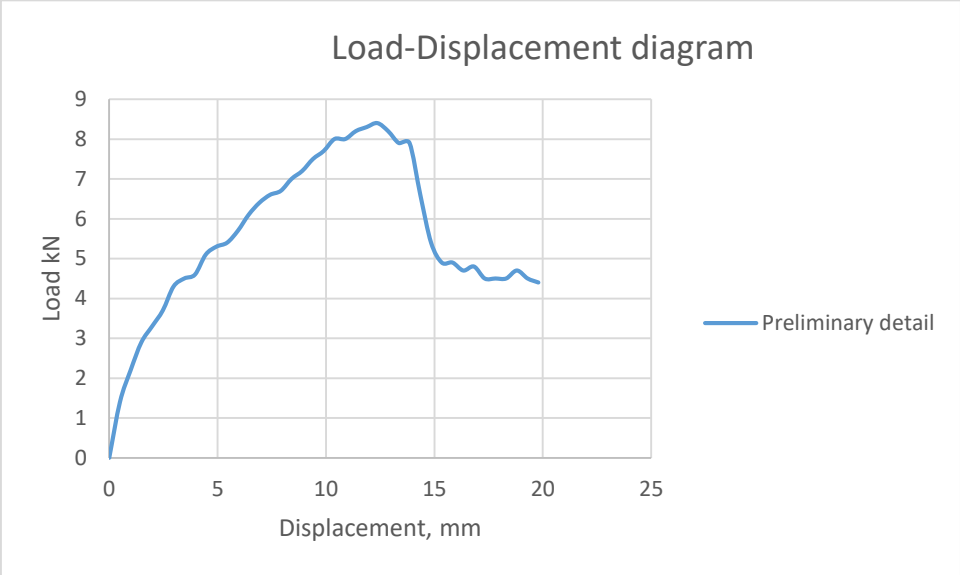

Figure 4. 15 Load displacemet diagram for preliminary joint

Cracking at the reentrant corner occurred when the normal tensile stress at the re-entrant corner was still lower than the effective tensile strength. This was because; the principal stress at the re-entrant corner reached the effective tensile strength, thus causing a crack to initiate at that corner, and tension-softening afterwards. With this illustration, it becomes clear that looking at normal stresses and strains (as done for B-regions) does not fully represent the behavior for D-regions. Thus, principal stresses and strains are very important parameters in this study.

After crack initiation, the crack propagated inwards into the section in an almost straight line, with the cracks concentrated around the reentrant corner. The joint was almost fully cracked after the application of a rather small load. The frame failed at 8.53kNm moment, with an efficiency of 41.3% (compared with the calculated sectional capacity of 20.3kNm in section 3.3). The reason is that there was no diagonal reinforcement to resist the diagonal tensile force in the corner and the compressed concrete outside the tensile reinforcement is therefore pushed off as shown in Figure 4.16 a; it is comparable to the crack pattern found on Nilsson (1973) in Figure 4.16b. When this occurred, the compressive zone suddenly disappeared and the corner failed in a very brittle manner. The presence of L-shaped reinforcement around the outside of the corner serves little purpose since this reinforcement normally is compressed and, therefore, cannot prevent failure of the corner. Instead, it might even have a negative effect since it may assist in pushing the corner off. Hence, such a corner without any diagonal reinforcement, depends only on the resistance of the concrete tensile strength to counteract the tensile force *R*; thus, using more reinforcement on either the tensile or compressive sides is of little help.

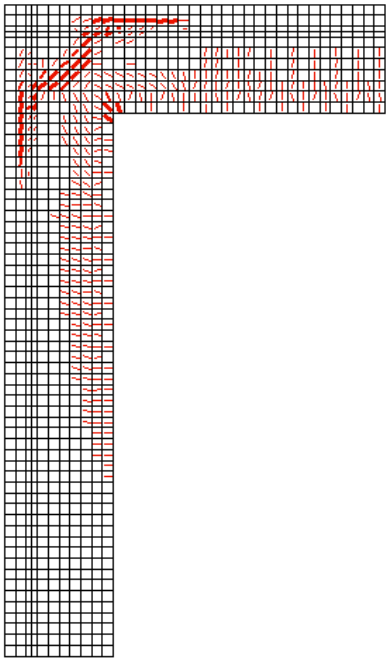

a)

b)

Figure 4. 16 a) crack pattern for the preliminary model b) crack pattern for such reinforcement according to Nilsson (1973)

4.3.2 Focus on thesis variants

This section reports on a study carried out on the four structural details that are shown below in Figure 4.17. These details are recommended in Eurocode 2, thus a proper understanding of their behavior and performance could prove useful to structural safety. The same geometrical dimensions will be adopted for all the cases. The difference however can be seen in the reinforcement layout at the joint region. In this section, perfect bond is assumed to exist between the reinforcement and the surrounding concrete.

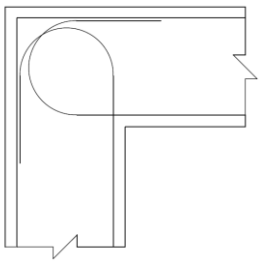

a) RL1

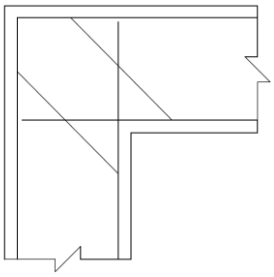

b) RL2

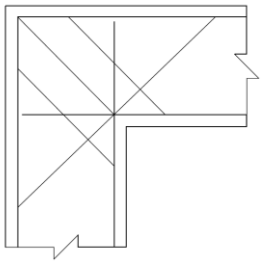

c) RL3

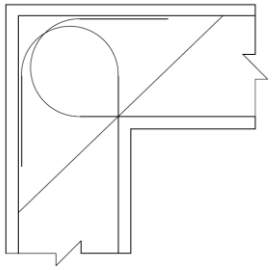

d) RL4

Figure 4. 17 Evaluated structural details for corner joints.

The corner joints in Figure 4.17 will be subsequently referred to as (a) Reinforcement Layout 1, RL1, (b) Reinforcement Layout 2, RL2 (c) Reinforcement Layout 3, RL3 and (d) Reinforcement Layout 4, RL4. The goal of this section is to understand how joints with these structural details behave by examining its stresses and strains, failure mode and joint efficiency.

4.3.2.1 Reinforcement layout 1 (RL1)

An old way of placing reinforcement in a corner is to form it into a loop. Detailing system RL1 is a more practical reinforcement layout, as it is easier to assemble on site. It is achieved through the use of two bent bars; the bar in each leg of the specimen is brought well inside the corner and then bent back into the compression zone of the same leg. This detail offers the advantage that the two bent bars enclose the corner with reinforcement. The structural detail is illustrated in figure 4.17a. This reinforcement layout attained a peak moment of 11.76 kNm, thus 57.9% joint efficiency for the design moment (reference moment is 20.3 kNm).

The behavior is summarized is as follows: The cracking was initiated at 1.8kNm. Crack initiated at this load step because the maximum principal stress, σ_1 reached the material tensile strength of 1.35MPa. After crack initiation, the material behavior is increasingly non-linear as the cracks grew. The concrete near the re-entrant corner softened in tension and inner concrete carried more tension. Thus, cracks propagated inwards. At the failure moment of 11.76kNm, cracking with in the joint caused a premature Failure. This cracking was initiated by the transverse tension within the inclined strut (the largest tensile strain occurred along the strut (the red contours in Figure 4.18)).

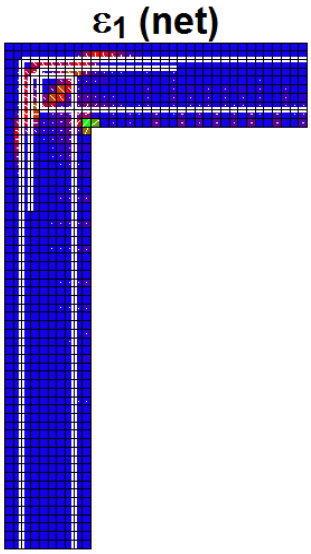

Figure 4. 18 Maximum principal strain, ε_1

For this detailing, the crack in the model was initiated at the re-entrant corner and on subsequent loading, the crack travelled along the corner diagonal for some distance and then branched out into numerous cracks progressing towards the compression zone of the corner following the loop. The final stages were marked by the appearance of a crack near the exterior portion of the corner of the joint aligned more or less perpendicular to the corner diagonal. The cracking around the loop reduced the anchorage and consequently the load carrying capacity decreased. The crack pattern is shown in Figure 4.19 below.

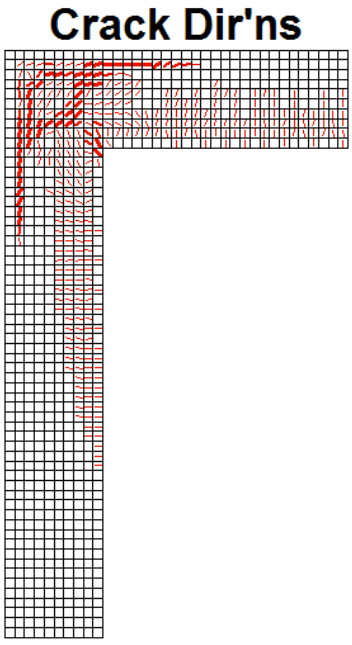

Figure 4. 19 Crack pattern at Failure, RL1

4.3.2.2 Reinforcement layout 2 (RL2)

In the structural detail shown on Figure 4.17b, inclined stirrups are added to the straight tensional reinforcement. The use of such radial reinforcements substantially improved the structural behavior of the corner, resulting in a considerable increase in efficiency. Nevertheless, even though this detailing gave considerably improved behavior, it did not attain full efficiency. This reinforcement layout attained a peak moment of 17.54kNm, thus 86.4% joint efficiency for the design moment (reference moment is 20.3 kNm) was achieved.

The behavior is summarized as: The cracking was initiated at 1.68 kNm. Crack initiated at this load step because the maximum principal stress, $\sigma_{1,}$ reached the material tensile strength of 1.35Mpa. At that cracking load, The compressive stress in the strut is elevated at the ends, and quite uniform in the middle part. On the other hand, tensile stress is largest in the middle of the inclined strut.

At the peak moment of 17.54kNm, the concrete strains of the structure was only 1.35‰. But the reinforcement stress reached 347.8MPa, hence it yielded. The tensile reinforcement inside the joint yielded consequently the concrete crushed on the next load step with strain reaching 10‰.

In summary, Failure was primarily caused by the yielding of reinforcement in the joint. Secondary diagonal tension crack failure and compression failure occurred as a consequence. The crack pattern at failure is shown in Figure 4.20 below.

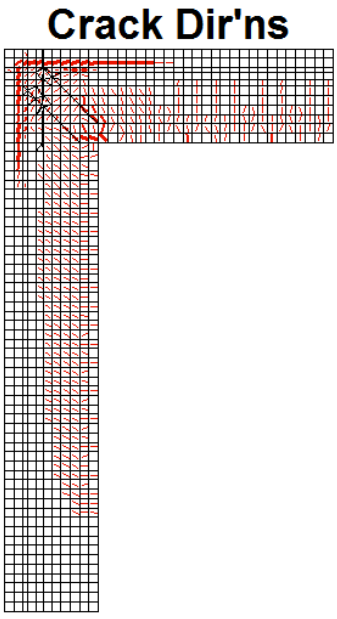

Figure 4. 20 Crack pattern at Failure, RL2

Significant improvements in behavior were observed in model RL2 compared to RL1. The stirrups were apparently effective in carrying a significant amount of diagonal tension and the joint efficiency increased to 86.4%. The crack widths at service loads were reduced and there was a decrease in the extent of cracking. It may by noted that the joint efficiency was still below 100% in spite of the provision of a primary diagonal tension-resisting element in the form of stirrups.

4.3.2.3 Reinforcement layout 3 (RL3)

With this detailing shown on Figure 4.17c, an ultimate moment of 30.1kNm was achieved. This ultimate moment attained a joint efficiency of 100.3% when compared to the design strength of the member (i.e. $29.95kNm$). In addition, unlike all the joints studied earlier, failure did not occur in the joint, Rather flexural failure occurred in the beam.

Cracking occurred when the maximum principal stress, σ_1 reached the concrete tensile strength, with the cracking moment being $2.1kNm$. The presence of the diagonal bar did not alter the stress distribution at this load level. Thus, there was still tensile stress concentration at the re-entrant corner. The cracking moment value is marginally larger than the other variants because the addition of the diagonal bar slightly increased the second moment of area of the section around the re-entrant corner. Thus, the addition of diagonal bar had negligible influence prior to cracking. Its influence increased in significance after cracking has been initiated at the re-entrant corner. After cracking, the steel was activated and the impact of the diagonal bar grew with as the load increased.

At the failure moment of 30.1kNm the steel stress reached 347.8Mpa, hence it yielded. However, the concrete strains of the structure was only 1.4‰, thus concrete failure did not occur. This detail prevented diagonal tension failure.

With the diagonal bar placed at approximately 45°, it provided strength and stiffness that enabled the frame corner to cope better with the stress field at that location. While transverse tension still caused cracking within the inclined strut, the stirrups that crossed the strut were effective in controlling the crack width. This made the inclined strut stronger, stiffer and less susceptible to compressive strain. Failure occurred due to the flexural cracks that propagated into the beam, which led to flexural failure of the beam. Hence in this detail, failure at the joint was avoided.

The largest magnitude of compressive strain at failure, occurred along the beam member length as seen in Figure 4.21, flexural cracks are formed in the beam. The joint is not governing in this case, and does not prevent the connected members from reaching their capacity.

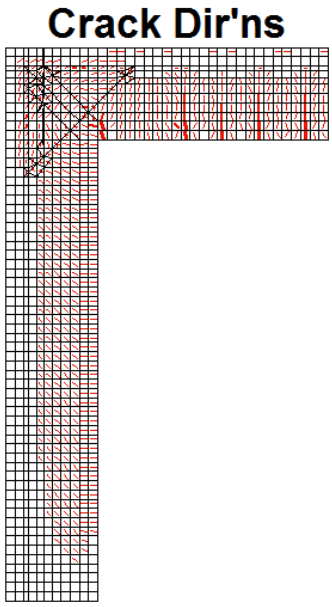

Figure 4. 21 crack pattern at failure, RL3

4.3.2.4 Reinforcement layout 4 (RL4)

Detail RL4 is a modification of RL1 by adding diagonal bars to the loop reinforcement. The structural detail is illustrated in Figure 4.17d. This reinforcement layout attained a peak moment of 15.68 kNm, thus approximately 52.3% joint efficiency for the design moment (reference moment is 29.95 kNm).

The observed behavior is summarized as follows: The cracking was initiated at 2.1kNm. After crack initiation, the material behavior is increasingly non-linear as the cracks grew. The concrete near the re-entrant corner softened in tension and inner concrete carried more tension. Thus, cracks propagated inwards. At the failure moment of 15.68 kNm, the concrete strains of the structure exceeded 3.5‰. Failure occurred due to crushing of concrete along the strut.

In this reinforcement arrangement due to the 180° bend bars, it presents a certain amount of reinforcement perpendicular to the diagonal tension crack. Further, when the reinforcement is tensioned at the inside, the loops confined the concrete, and hindered the formation of a crack inside the loop. Hence, the reinforcement loops forced the diagonal crack out in the corner where the tensile stresses are less pronounced. Instead of forming a diagonal crack within the corner, the cracks then follow the loops until close to the compressive reinforcement, at which point they deviate in the direction of the adjoining members. Eventually, the cracks propagate as shown in Figure 4.22 and the concrete outside the reinforcement is pushed off. The anchorage of the loops is then reduced and the load capacity decreases with increasing rotation of the loops. The crack pattern shown on Johansson (2001), resembles the one found in the finite element simulation.

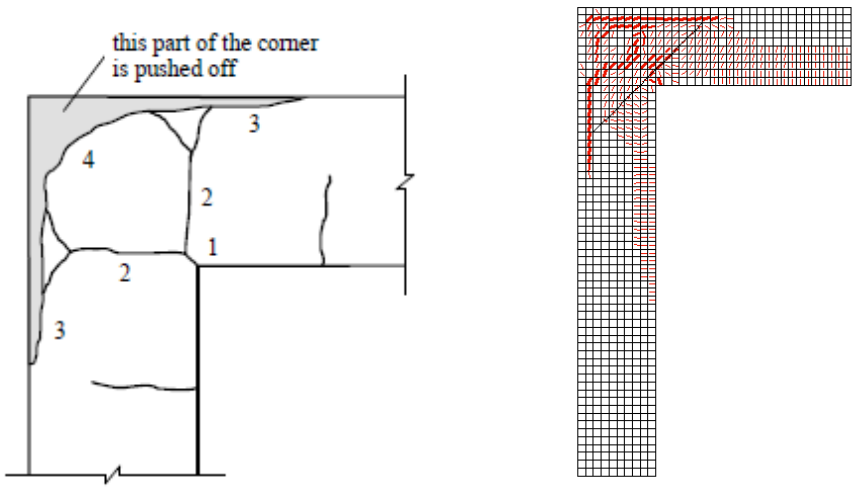

Figure 4. 22 a) crack pattern by Johansson (2001) b) crack pattern of RL4

4.3.3 Corner Joints with Chamfer

From the models evaluated, it is obvious that crack initiates at the reentrant corner at very low loads. It can be seen from Figure 4.23, a graph showing a comparison between the load at first crack and the ultimate load. One way to remedy this problem is by providing chamfer at the inner corner of joints. In the present subsection, corner joints are modelled to investigate the effect of chamfer.

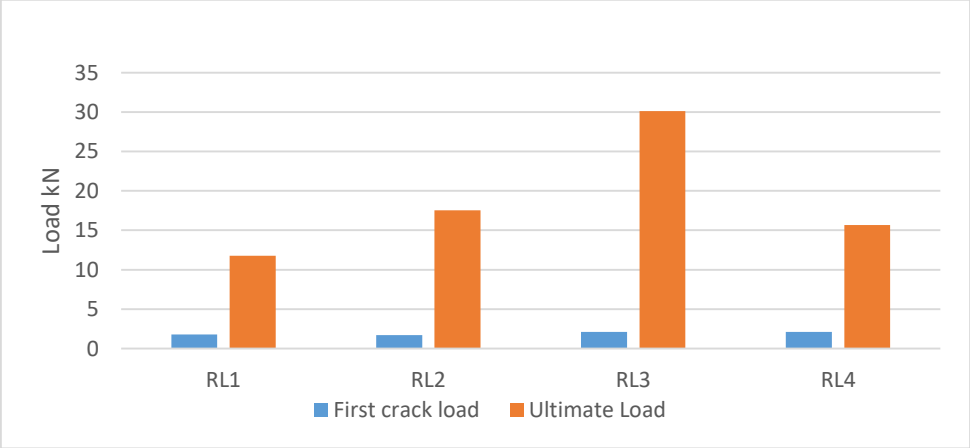

Figure 4. 23 comparison of load carrying capacity

On a study carried out by Dhar and singh (2004), a chamfer equal to the thickness of the framing member, with loop and inclined steel is recommended. Accordingly, three models with detailing system comprising of loop steel and inclined bars (same as RL4) were modelled on VecTor2. The chamfer sizes (L) considered are 100mm, 150mm and 200mm (the joints subsequently referred to as C-1, C-2 and C-3 respectively).The effect of chamfer size on the stress distribution in the corner joint was studied and the results are discussed.

Variation of σ_x along the diagonal: σ_x represents stress acting in the direction perpendicular to the diagonal as shown on Figure 4.23. In all the cases considered, the stress σ_x has maximum value at the inner corner and it is tensile in nature, this can be seen in Figure 4.24. From the diagrams, it is clear that σ_x reduces with the increase in chamfer.

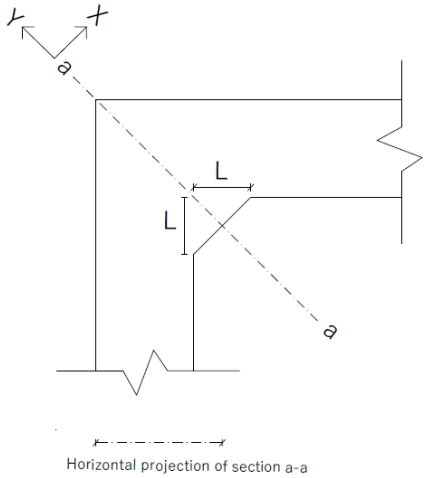

Figure 4. 24 Corner joint with chamfer

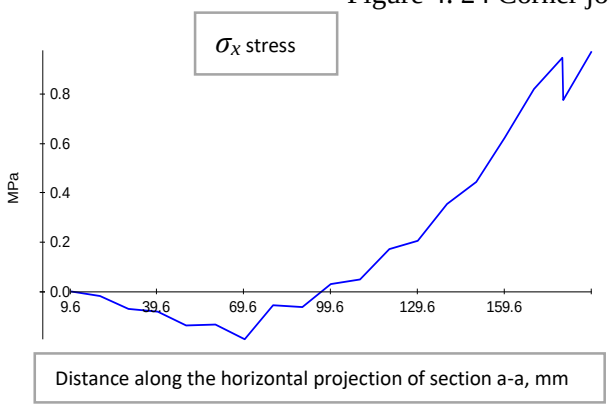

a) RL4

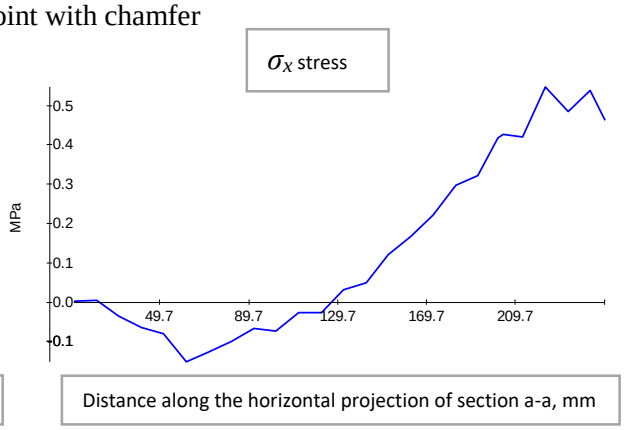

b) C-1

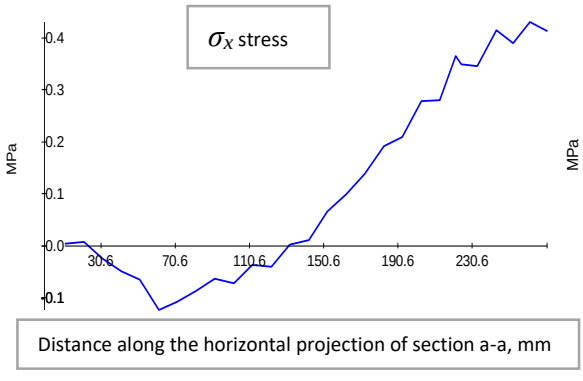

b) C-2

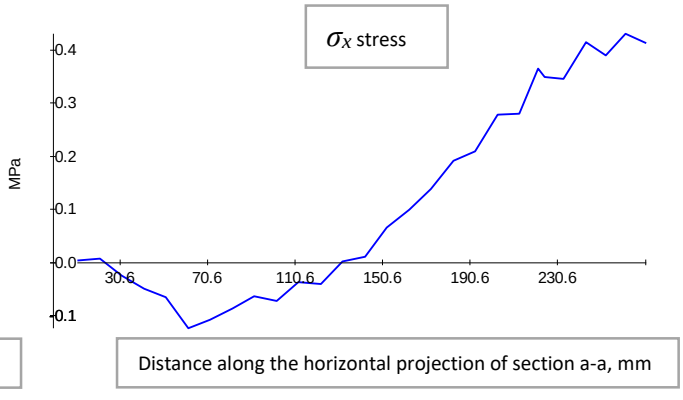

d) C-3

Figure 4. 25: variation of σ_x along the diagonal for varying chamfer sizes

The Load displacement diagrams of the corners with varying chamfer sizes are shown in Figure 4.26. The behavior of all the corners before cracking were similar. After the initiation of cracking, the joints behaved differently, with C-3 (the corner with 200mm chamfer) showing better performance.

The efficiency of the chamfered corners was calculated and shown in Table 4.7 below. While the cracking load in all four corners remained practically the same, the location of the first crack formation varied. The first crack formed either in the framing members or at the junction of the framing members with the chamfer. Figure 4.27 shows the location of the crack formation for the corners.

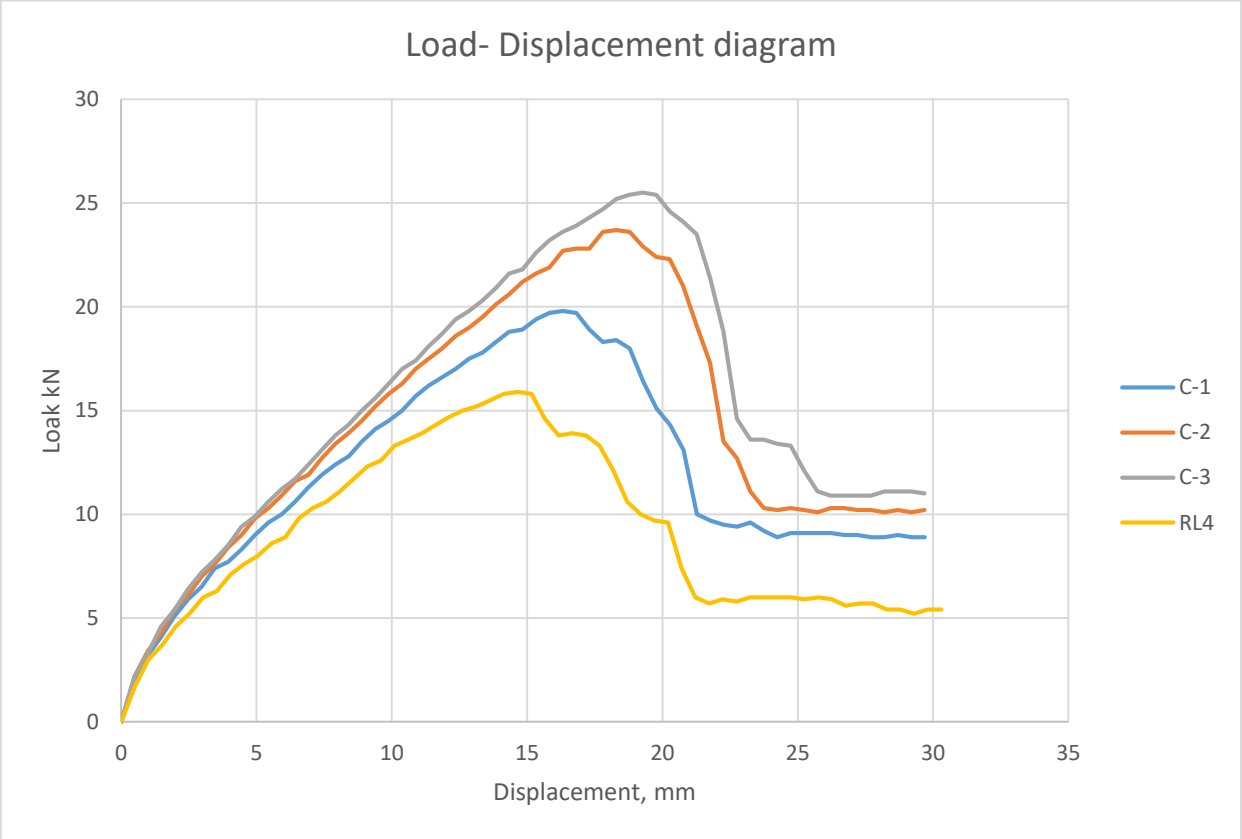

Figure 4. 26 Load displacement diagram of chamfered corners

Table 4. 7 Results of chamfered corners

Designation	Chamfer size, mm	Cracking Moment, kNm	Maximum σ_x, at 2.1kNm load	M_{uv}, Failure moment VecTor2	M_{cal}	Efficiency (%),M_{uv}/M_{cal}
RL4	0	2.1	0.978	15.68	29.95	52.3
C-1	100	2.1	0.55	19.4	29.95	64.7

C-2	150	2.1	0.414	23.3	29.95	77.4
C-3	200	2.1	0.4	24.9	29.95	83.1

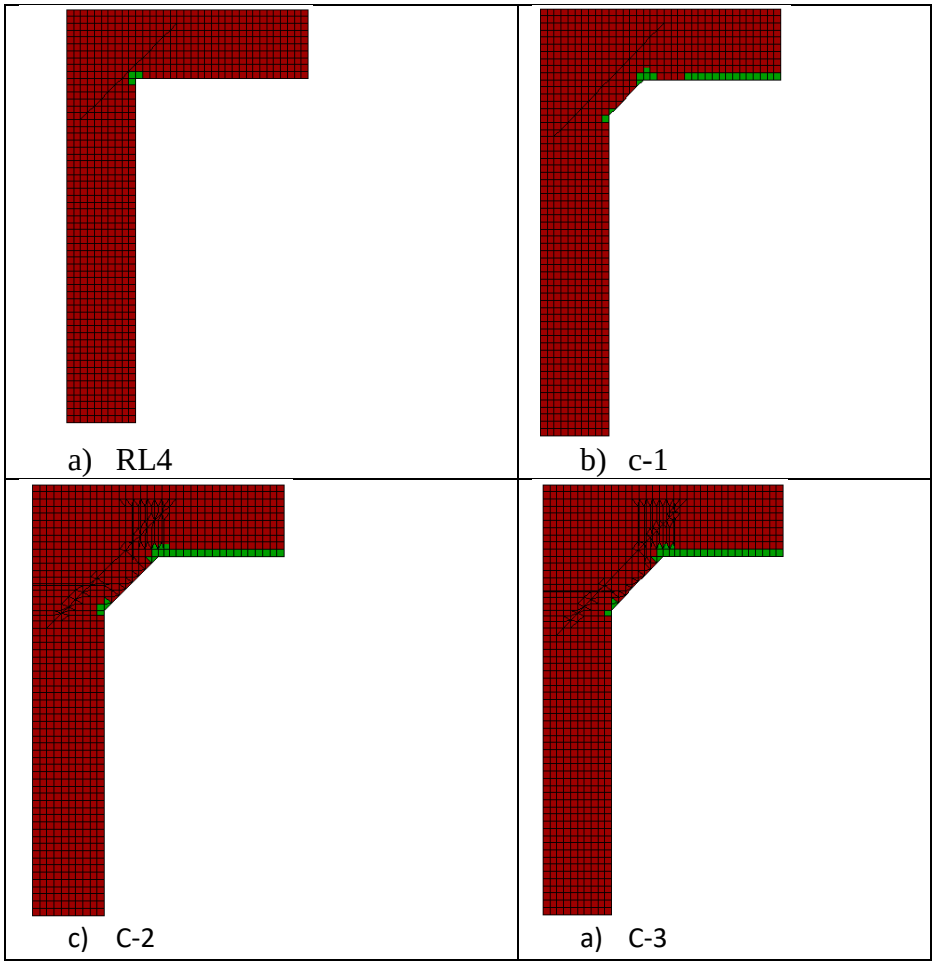

Figure 4. 27 Crack location of chamfered corners

In conclusion, failure load and joint efficiency increased with increase in chamfer. The overall stress level in the corner decreased with increase of chamfer size. In addition, it was observed that cracking in the corner region reduced with increase in chamfer.

4.3.4 Effect of reinforcement ratio

From previous studies, it can be understood that the tensile strength of concrete controls the behavior of opening corners which in turn governs percentage of tension steel. Hence the percentage of tension reinforcement in the corner has to be kept reasonably low in order to minimize overstressing of concrete in tension and reduce the chances of brittle tensile failure of concrete at relatively lower loads. Therefore, the reinforcement percentage in the specimen was varied to test the validity of the above hypothesis, a finite element study with respect to the effect

of the amount of tension reinforcement on performance of opening corners was carried out. Using the same arrangement of reinforcement shown in Figures 4.28-4.31, the four corners were designed. From Figure 4.28-4.31, the load Displacement diagram of detailing types RL1, RL2, RL3 and RL4 for various reinforcement ratio is shown.

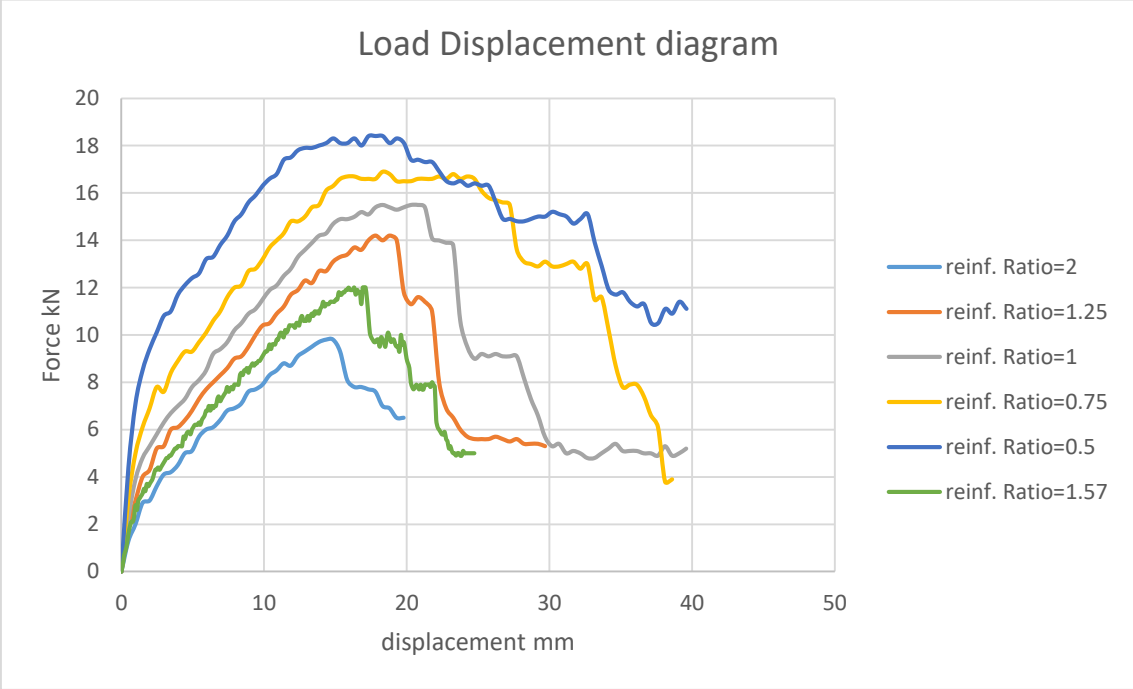

Figure 4. 28 Load Deflection relationship of RL1 with varying percentage of tensile reinforcement

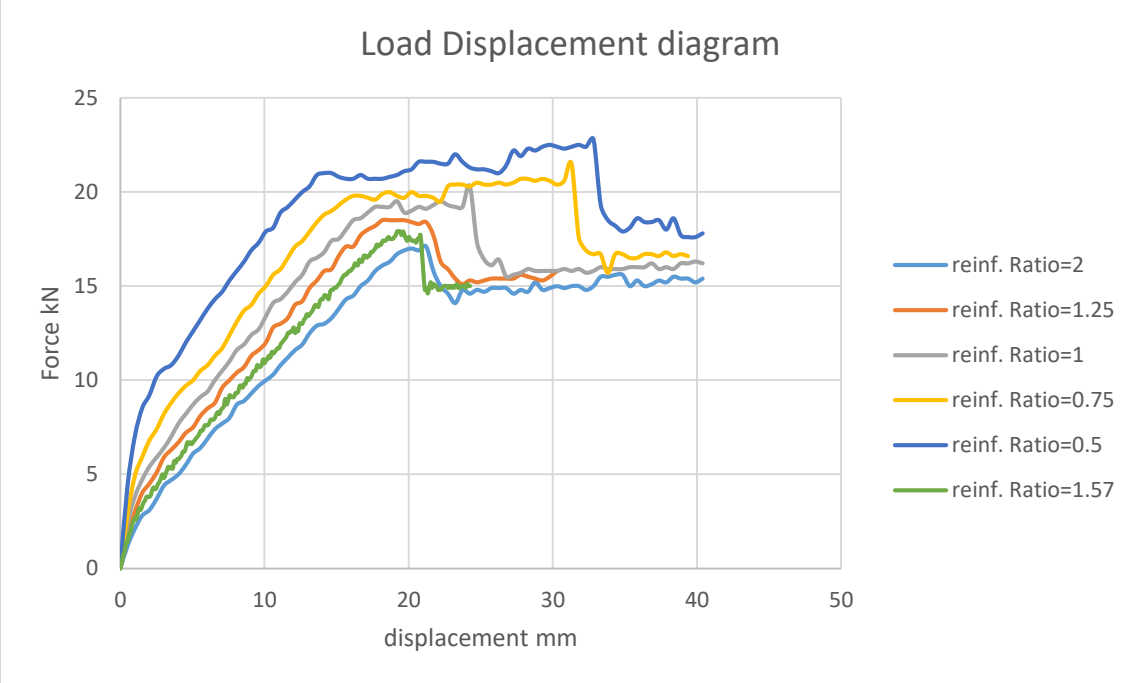

Figure 4. 29 Load Deflection relationship of RL2 with varying percentage of tensile reinforcement

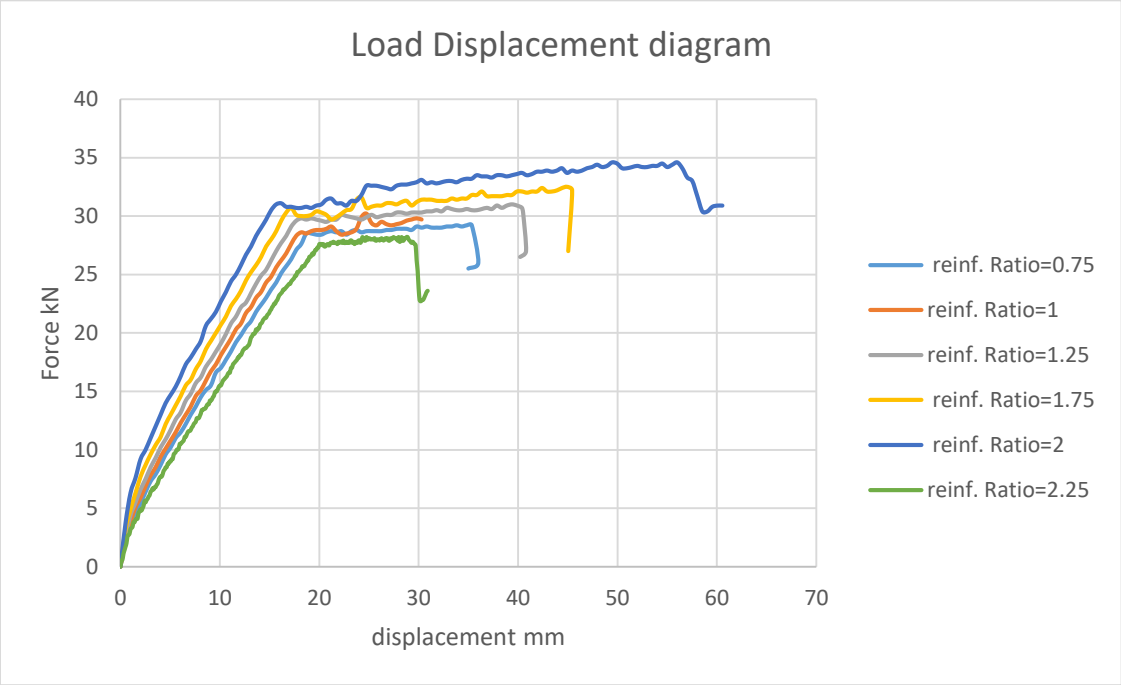

Figure 4. 30 Load Deflection relationship of RL2 with varying percentage of tensile reinforcement

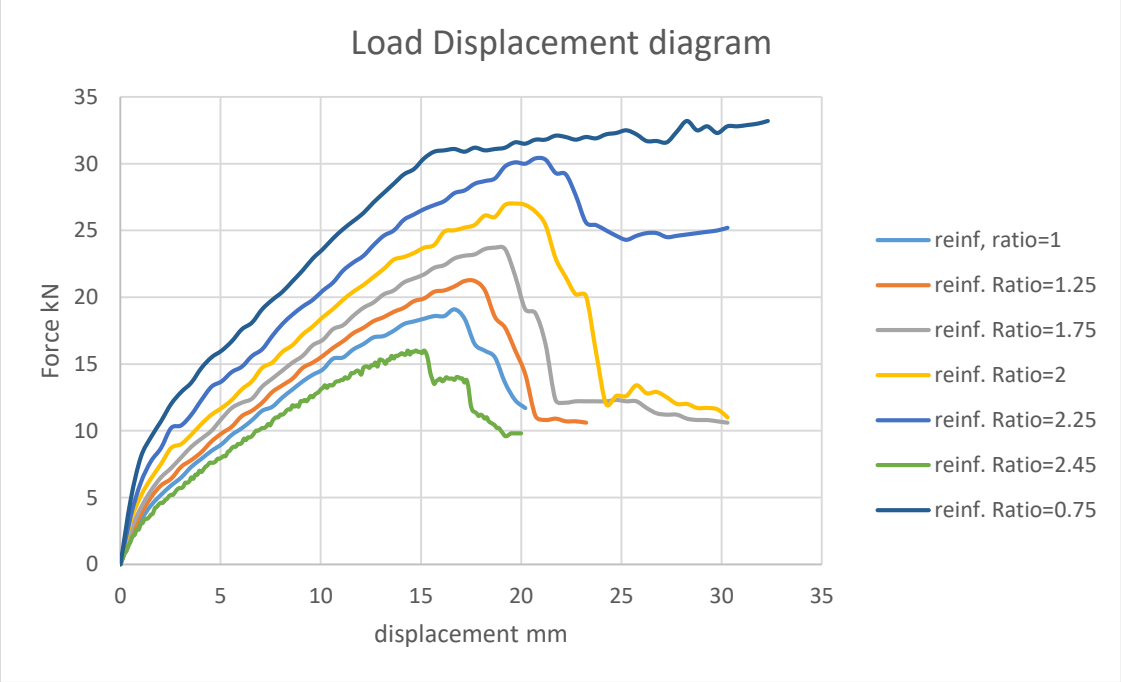

Figure 4. 31Load Deflection relationship of RL4 with varying percentage of tensile reinforcement

From the graphs above, it can be understood that joint efficiency increases as tensile reinforcement ratio decreases. This is more evident in the cases of RL1 and RL4 as compared to RL2 and RL3. Due to stirrups in RL2 and RL3, these details are less sensitive to large reinforcement ratios.

4.4 Discussions of results

The different steel reinforcement details of frames RL1-RL4, affect the crack patterns, cracking load and failure load. The confinement of frames RL2 and RL3 by means of stirrups improved the cracking behavior and increased the cracking and failure loads of these frames compared with RL1 and RL4. Owing to the fact that the stirrups confined the concrete of the joint, and hence reduced the possibility of the formation of the internal cracks within the joint. A satisfactory structural behavior was observed in reinforcement layout 3, RL3, by achieving an efficiency of 100.3%. The effect of diagonal steel on the behavior of the corner could be clearly seen and it is postulated that inclined steel stiffened the corner and delayed the widening and propagation of crack initiated at the reentrant corner of the joint.

Figure 4.30 and 4.31, are graphs showing the force-displacement for RL1 Vs RL2 and RL3 Vs RL4 respectively. The similarity in pre crack behavior shown on the graphs, shows that the joints behave essentially the same regardless of the reinforcement layout up till cracking. After cracking, the reinforcement layout determines the joint behavior. It can be clearly seen that RL2 had a much higher capacity as compared to RL1. Similarly, Even though members of both RL3 and RL4 detailing's have the same moment capacities, when loaded to failure, RL4 was only able to sustain almost half the moment it was designed for.

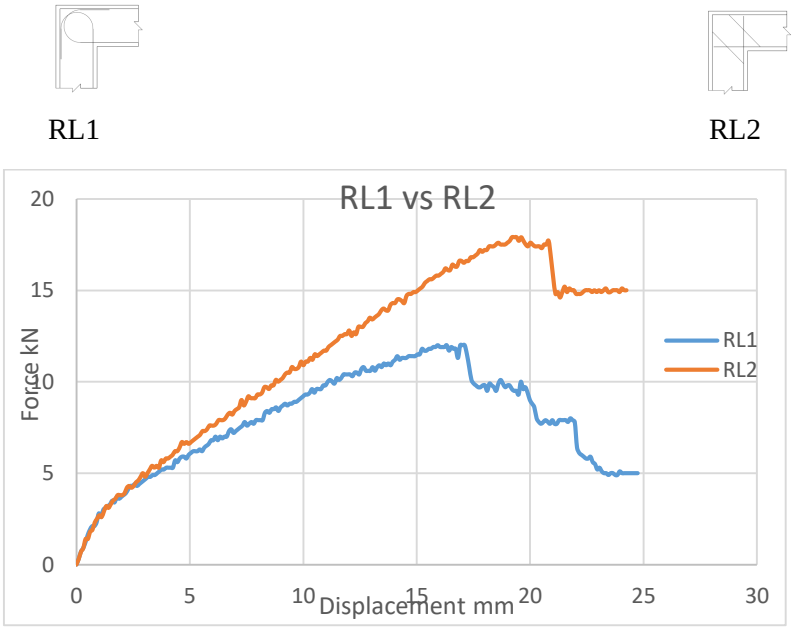

Figure 4. 32 Force-displacement diagram for RL1 and RL2

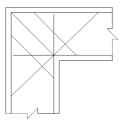

RL3

RL4

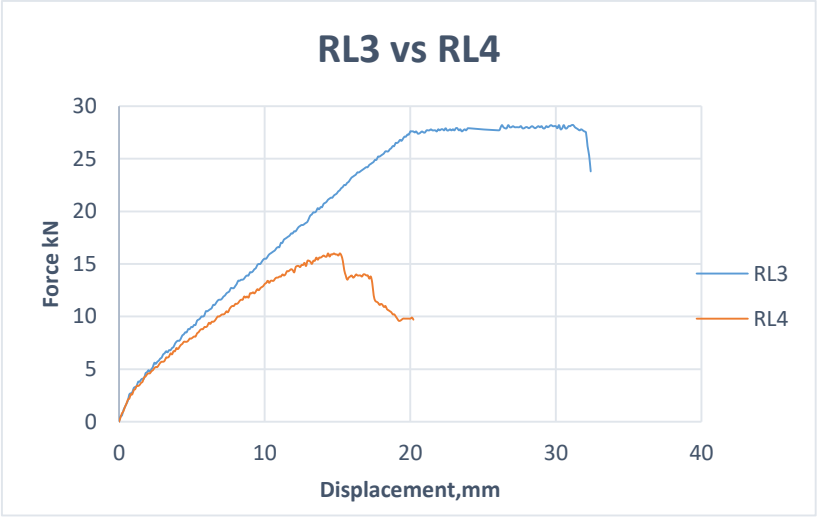

Figure 4. 33 Force-displacement diagram for RL3 and RL4

Based on the peak moments attained by the corner joints, RL1 achieved an efficiency of 57.9% while RL4 had an efficiency of 52.3%. Contrary to this, experimental investigations by different authors have found better efficiencies. Referring to Figure A.1 and A.2 in the Appendix, detailing similar to RL3 has an efficiency of 60-80%, while RL4 detailing showed superior performance with efficiency greater than 100%. So why did details RL1 and RL4 perform poorly, while literatures (Nilsson (1973), Johnsson (2000), (Roshan, 2015) and others) say otherwise? The reason is high reinforcement ratio. One may think that an increased reinforcement amount, and thereby, an increased moment capacity, will improve the structure. However, this is not always the case, since a large reinforcement amount may cause a brittle failure. Larger amounts of reinforcement imply larger inner forces to be deviated within the joint.

Eurocode has set a maximum 2% reinforcement ratio for RL1 detailing, While 2% is set as the minimum reinforcement ratio limit for detailing RL4. Accordingly 1.57% and 2.45% reinforcement ratios were used for RL1 and RL4 respectively. It can be established that, the performance of these joints is highly affected by reinforcement ratio. Due to that, these reinforcement details were unable to reach full capacity.

Why did reinforcement layout RL2 and RL3 perform better than RL1 and RL4 respectively, when similar reinforcement ratios were used? The answer is stirrups. Park and Paulay (1975),

Kaliluthin, Kothandaraman and Suhail-Ahamed (2014) etc. recommend increasing shear (transverse) reinforcement for medium to highly reinforced sections because, it would provide confinement to the concrete. Though the concrete could still crack, the concrete within the cracks would still contribute to performance of the joint via tension stiffening effect, hence reduce deformation in the section.

In summary, the recommended limits of the reinforcement ratio, ρ, in Annex EC2 J.2.3, concerning detailing of the reinforcement layout in frames subjected to an opening moment, are not appropriate, see Figure 2.14 and Figure 2.15 and Equation (2.8) and Equation (2.2), respectively. The high limit of the reinforcement amount can cause undesired response to occur. Hence the full corner efficiency will not always be reached and the failure might be brittle.

5. Conclusion and recommendation

5.1 conclusion

From the corner beam-column joints studied, the following conclusions are drawn.

- Design of corner joints can be consistently performed based on lower-bound solutions of the theory of plasticity such as the strut-and-tie models (STM).
- The structural response of frame corners subjected to opening moments can be reliably captured to as significant degree of accuracy with the use of nonlinear finite element analysis.
- Opening corners may potentially present poor performance and a rather brittle behavior at failure. The behavior and strength of such members is highly influenced by the reinforcement layout and tensile reinforcement ratio.
- The efficiency of corner joints decrease for increasing amount of tensile reinforcement ratio.
- The 2% limit on reinforcement ratio on Eurocode seems to be exaggerated, and due to this high reinforcement ratio specified, the looped reinforcement layouts were not able to reach full capacity.
- Providing transversal reinforcement (stirrups) in the joint, improves the joint regions performances both in terms of strength and deformation capacity significantly.
- The anchoring of the tensile reinforcement by stirrups and diagonal bars leads to a better overall cracking behavior of the corner, and more significantly, to the reduction of the dangerous diagonal tension splitting cracks of the corner.
- Tensile stresses inside a corner joint reduce considerably with the increase in chamfer. In addition failure load and joint efficiency increase with the increase in chamfer.

5.2 Recommendation

- More research should be done on acute and obtuse angles subjected to opening moments.
- Section with different height of cross-section should be studied, as it is not included in the Eurocode and appears rarely in publications.
- Further study should be done by adding steel fibers to the joint region, as cracking plays a major role in the capacity of joints.

References

Abdul-Wahab, H.M.S and Al-Roubai, A.A.M. (1998). Strength and behavior of steel fibre reinforced concrete corners under opening bending moment. Magazine of Concrete Research,

AL-khafaji, J.M., AL-bayati, Z.A., AL-mallki, A.A.K. (2011) Experimental Study of R.C. Corner Details. Al-Qadisiya Journal for Engineering Sciences, Vol. 4(1), pp. 516-531.

Bahn, B.Y. and Hsu, T.T.C. (1998) Stress–strain behavior of concrete under cyclic loading. ACI Material Journal. Title No. 95-M18: PP 178–193.

Balint and Harold P. J. Taylor (1972), Reinforcement Detailing of Frame Corner Joints with Particular Reference to Opening Corners, Technical Report 42.462, Cement and Concrete Association, London

Beer, F.P., Johnston, E.R., DeWolf, J.T., and Mazurek, D.F. (2011). Statics and Mechanics of Materials. McGraw-Hill, New York

Bhatt, P., MacGinley, T.J. and Choo, B.S (2014). Reinforced concrete design to eurocodes - Design theory and examples. 4th edition. CRC Press. Boca Raton, Florida.

M.D. Brown and Oguzhan Bayrak., (2008). Design of Deep Beams Using Strut-and-Tie Models—Part II: Design Recommendations. ACI Structural Journal, V. 105, No. 4, pp 142-149.

Calavera, J. (2012). Manual for Detailing Reinforced Concrete Structures to EC2. Spon press, London.

Campana, S., Ruiz, M.F. and Muttoni, A. (2013). Behavior of nodal regions of reinforced concrete frames subjected to opening moments and proposals for their reinforcement. Engineering Structures 51 pp 200–210.

CEB (1996). RC Frames under Earthquake Loading: State of the Art Report. Thomas Telford, London.

Cook, R.D., Malkus, D.S., Plesha, M.D. and Witt, R.J. (2002). Concepts and applications of finite element analysis, 4th Edition. John Wiley & Sons Inc. New York.

Cunningham, L.S (2000). Automatic Design of Concrete Structures Using a Strut & Tie Approach. Ph.D Thesis. University of Glasgow.

Dahlgren and Svensson (2013). Guidelines and Rules for detailing of reinforcement in concrete structures, Chalmers University of technology, master's thesis 2013:142

V.N Dhar,. And Dr. Singh, R.P. (2004), "Chamfering and Reinforcement Detailing in Reinforced Concrete Corner Subjected to Opening Moment", IE (I) Journal-CV Volume 84, Feb., 244-251.

Eurocode 2 - Concrete structure - Part 1-1: General rules and rules for buildings

Hendy, C.R. and Smith, D.A. (2007). Designers' Guide to EN1992-2: Eurocode 2: Design of concrete structures part 2, concrete bridges. Thomas Telfords, London. 139

Foster J, Gilbert RI. (1996). The design of non-flexural members with normal and high strength Concretes. ACI Struct J;93(1):3–10.

Hsu, T.T.C. and Mo, Y.L. (2010). Unified Theory of Concrete Structures. John Wiley and Sons, West Sussex, UK

Johansson, M. (2000), Nonlinear Finite-Element Analyses of Concrete Frame Corners Journal of Structural Engineering, Vol. 126(2), pp. 190-199.

Johansson, M. (2001), Reinforcement detailing in concrete frame corners, ACI Structural Journal, Vol. 98(1), pp. 105-115.

Kaliluthin, A.K., Kothandaraman, S. and Suhail-Ahamed, T.S. (2014). A Review on Behavior of Reinforced Concrete Beam-Column Joint. International Journal of Innovative Research in Science, Engineering and Technology, Vol. 3, Issue 4

Kassem, w. (2014). Strength Prediction of Corbels Using Strut-and-Tie Model Analysis. International Journal of Concrete Structures and Materials. Vol.9, No.2, pp.255–266.

S.K. Kaushik, B. Singh, (2003). Investigations on fiber reinforced concrete opening corners, IE (1) J.-CV 84 201–209.

Luo, Y.H., Durrani, A.J., Shaoliang, B., Yuan, J. (1994) Study of Reinforcing Detail of Tension Bars in Frame Corner Connections. ACI Structural Journal, Vol. 91(4), pp. 486–496.

MacGregor, J.G. and Wight, J.K. (2005). Reinforced Concrete Mechanics and Design. 4th edition. Prentice Hall, Upper Saddle River, New Jersey.

Marti, P (1985). Basic Tools of Reinforced Concrete Beam Design, ACI Journal, Proceedings V. 82, No. 1, pp. 46-56.

Mayfield, B., Kong, F. K., Bennison (1972). A. Strength and Stiffness of Lightweight Concrete Corners. ACI Journal, Vol. 69(7), pp. 420–427.

Mosley, B., Bungey, J. and Hulse, R. (2012). Reinforced Concrete Design to Eurocode 2. Palgrave Macmillan, Hampshire, United Kingdom.

Moretti, M., Tassios T. and Vintzileou (2014). Behavior and design of corner joints under opening bending moment, ACI Journal

Mörsch, E (1909). Concrete-Steel Construction, E. P. Goodrich, translation McGraw-Hill, New York, 1909, 368 pp.

Muttoni, A., Schwartz, J. and Thurlimann, B. (1997). Design of Concrete Structures with Stress Fields. Birkhauuser verlag, Basel, Switzerland.

Muttoni A, Schwartz J, Thürlimann B. (1996). Design of concrete structures with stress fields. Basel, Switzerland: Birkhäuser Verlag;

Muttoni, Fernández Ruiz M (2007). Development of suitable stress fields for structural concrete. ACI Structural journal 104(4):495–502.

Nabil, M., Hamdy,O. and Abobeah, A. (2014). Affecting aspects on the behavior of frame joints. HBRC Journal

Nilson, A.H., Darwin, D. and Dolan, C.W. (2004). Design of Concrete Structures. 14th edition. McGraw-Hill, New York.

Nilsson, I.H.E. (1973). Reinforced concrete corners and joints subjected to bending moment: design of corners and joints in frame structures. Document D7:1973, National Swedish Institute for Building Research, Stockholm.

H. E. Nilsson and A. Losberg, (1976). Reinforced Concrete Corners and Joints Subjected to Bending Moment, Proceedings ASCE, Journal of the Structural Division, Vol. 102,
, pp. 1229–1254.

S. Park, K. Mosalam (2012). Experimental investigation of non-ductile reinforced concrete corner beam-column joints with floor slabs, J. Struct. Eng., ASCE 139, 1–14.

Park, R. & Paulay, T. (1975). Reinforced Concrete Structures, 1st edition, John Wiley & Sons, New York.

Saeed A., Shah. A., (2009). Evaluation of Shear Strength of High Strength Concrete Corbels using Strut and Tie Model. TheArabian Journal of Science and Engineering, Vol.3 4(2B) pp 27-35.

Saeed A., Shah. A, Zaman S., (2009), Evaluation of the shear strength of four piles caps, using Strut and Tie Model. Journal of Chinese Institute of Engineers Vol.32 (2) pp.243-250.

Schlaich, J., Schafer, K. and Jennewein, M. (1987). Towards a consistent design for structural concrete. PCI Journal. V. 32(1987), No. 3, pp. 75-150.

Schlaich, J. and Schafer, K. (1991). Design and detailing of structural concrete using strut-and-tie models. The Structural Engineer, Vol 69, No. 6.

Shah, A., Haq, E. and Khan, S. (2011). Analysis and Design of Disturbed Regions in Concrete Structures. Procedia Engineering Journal – Elsevier. Volume 14, PP 3317–3324.

Skettrup, E., Strabo, J., Andersen, J.H., brondum-nielsen, T (1984). Concrete Frame Corners. ACI Journal, pp. 587–593.

Stroband J. and Kolpa J.J. (1981). The Behavior of Reinforced Concrete Column-to-Beam joints, Part 2: Corners Subjected to Positive Moments, Stevin Laboratory, Delft University of Technology, Report 5-81-5, Delft, The Netherlands

Stroband J. and Kolpa J.J. (1983). The behavior of reinforced concrete column-to-beam joints, Part 1, Corners subjected to negative moments. Stevin Laboratory, Delft University of Technology, Report 5-83-9, Delft, the Netherlands.

Tjhin, T.N. and Kuchma, D.A. (2002). Computer-Based Tools for Design by Strut-and-Tie Method: Advances and Challenges. ACI Structural Journal, Title no. 99-S60.

Torrenti, J.-M., Pijaudier-Cabot, G. and Reynouard, J.-M. (2010). Mechanical behavior of concrete. John Wiley and Sons, London

Vecchio, F.J. (1990), "Reinforced concrete membrane element formulations", J. of Structural Engineering, ASCE, 116(3), 730-750.

Vecchio, F.J. (2000), "Disturbed stress field model for reinforced concrete: Formulation", Struct. J., 126(9), ASCE, 1070-1077.

Vecchio, F.J. (2002), "Contribution of nonlinear finite element analysis to evaluation of two structural concrete failures", J. Performance of Constructed Facilities, ASCE, 16(3), 110-115.

Vecchio, F.J. and Bucci, F. (1999), "Analysis of repaired reinforced concrete structures", J. of StructuralEngineering, ASCE, 125(6), 644-652.

Vecchio, F.J. and Collins, M.P. (1986), "The modified compression field theory for reinforced concrete elements subjected to shear", ACI J., 83(2), 219-231.

Wong, P.S.L. (2002), "User facilities for 2D nonlinear finite element analysis of reinforced concrete", M.A.Sc. Thesis, Dept of Civil Engrg, Univ. of Toronto, 1-213.

Appendix

A. Effect of reinforcement ratio on corner efficiency

Macgregor (2005) compares the measured efficiency of a series of corner joints reported in H. E. Nilsson and A. Losberg, (1976) and P. S. Balint and Harold P. J. Taylor (1972) in figure A1. The *efficiency* is defined as the ratio of the failure moment of the joint to the moment capacity of the members entering the joint.

The solid curved line corresponds to the computed moment at which diagonal cracking is expected to occur in such a joint. Typical beams have reinforcement ratios of about 1 percent. At this reinforcement ratio, the joint details shown in Figure A-1 d and e can transmit at most 25 to 35 percent of the moment capacity of the beams. Nilsson and Losberg(1976) have shown experimentally that a joint reinforced as shown in Figue A-1b will develop the needed moment capacity without excessive deformations.

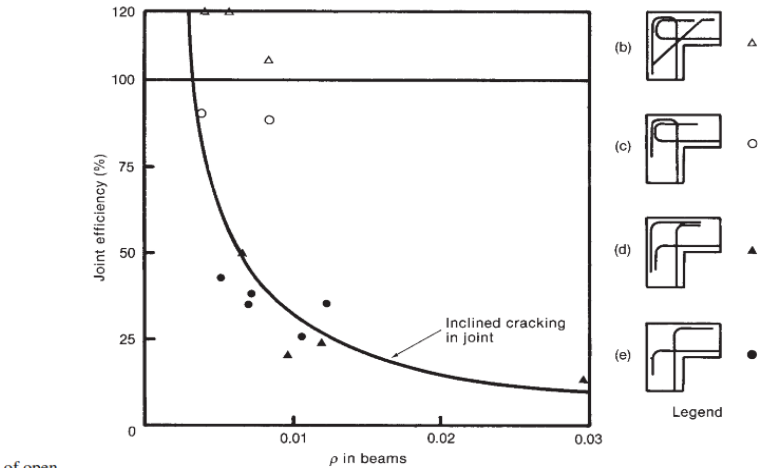

Figure A. 1 Relationship between measured efficiency and reinforcement ratio of opening joints (Macgregor, 2005)

Additionally, In Figure A.2 the result from tests on concrete frame corners performed by a number of researchers is summarized by Dahlgren and svensson (2013). The efficiency of different corners were compared with the mechanical reinforcement ratio, ϖ_s .

$$\varpi_s = \rho \frac{f_y}{f_c}$$

f_c cylinder compressive strength

f_y yield strength of the reinforcement

ρ reinforcement ratio

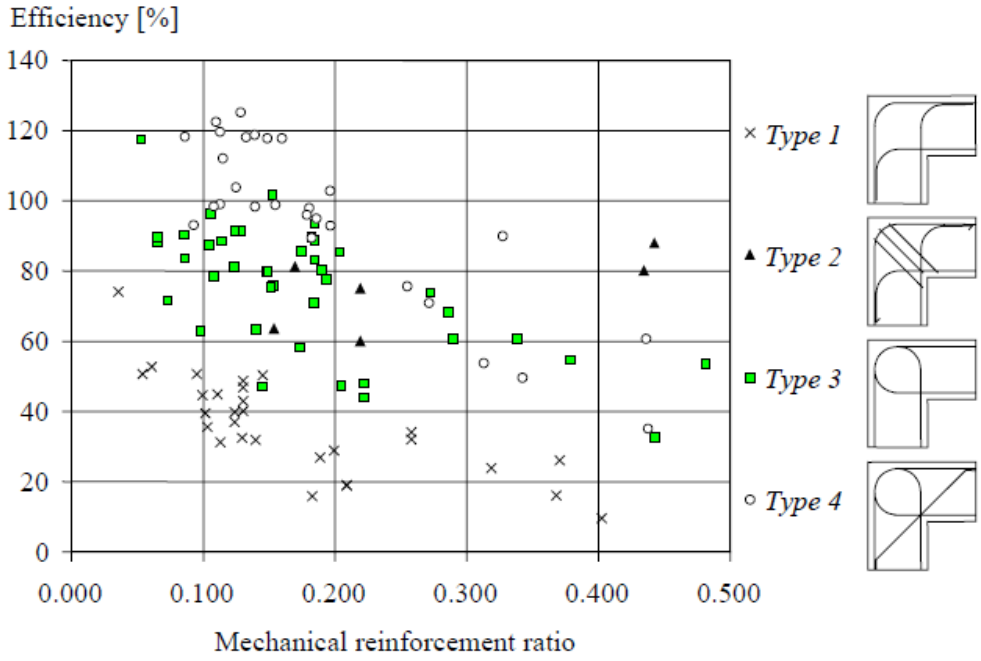

Figure A. 2 Efficiency of reinforcement detailing in frame corner subjecting to opening moment. (Dahlgren and svensson, 2013)